Multi-omics Reveal the Enabling Factors of Aplastic Anaemia

Xiaoyu Zhao
Tianjin Medical University
Chaomeng Wang
Tianjin Medical University
Chenchen Liu
Tianjin Medical University
Nan Jiang
Tianjin Medical University
Shaoxue Ding
Tianjin Medical University General Hospital
Yingying Chen
Tianjin Medical University
Liping Yang
Tianjin Medical University
Chunyan Liu
Tianjin Medical University General Hospital
Rong Fu (furong8369@tmu.edu.cn)
Tianjin Medical University General Hospital

Research Article

Keywords: macrogene CG-MS,, lipid metabolism, aplastic anaemia, Citrobacter, stearic acid, long-chain polyunsaturated fatty acids

Posted Date: February 4th, 2022

DOI: https://doi.org/10.21203/rs.3.rs-1313352/v1

Abstract

Background: Aplastic anemia is a kind of anemia caused by bone marrow failure due to autoimmune abnormalities. Numerous studies have shown that autoimmunity is regulated by intestinal microflora, and that most intestinal microflora regulates immunity through short chain fatty acids. At the same time, almost all patients with aplastic anemia will have bone marrow adipose tissue, and the process of bone marrow adipose tissue is regulated by medium and long chain fatty acids. Our previous studies have found that the intestinal flora of aplastic anemia patients is different from that of normal people. Therefore, this study aims to conduct a comprehensive detection of the intestinal flora and fatty acid metabolism in patients with aplastic anemia and to study their correlation.

Methods: Fatty acid compositions in the peripheral plasma and bone marrow supernatants of 12 newly diagnosed aplastic anaemia patients and 10 normal controls were comprehensively analysed by CG-MS. Gene sequencing of faecal samples from both groups was also performed with macrogene sequencing technology.

Results: Based on the metagenomic sequencing technology, we analyzed the difference of intestinal flora between group AA and group NC. We found that the main difference between the two groups existed in the bacterial community, and the abundance of most microbial species showed a downward trend. Based on the CG-MS lipid detection technique, we found that there were differences in lipid metabolism between the AA group and the NC group, whether short chain fatty acids or medium and long chain fatty acids. 8. The most attractive findings are interrelationships between the Citrobacter spp stearic acid (c18:0), isobutyric acid, and lysine degradation and betaine biosynthesis pathway and the interrelationship between catenibacterium_mitsuokai species at Catenibacterium, cis-7,10,13,16-docosatetraenoic acid (c22:4), ubiquinone and other terpenoid quinones pathway.

We also found the intercorrelation between the abundance of Enhydrobacter genus and Enhydrobacter_aerosaccus species, cis-13,16-docosadienoic acid in peripheral plasma, cis-7,10,13,16-docosatetraenoic acid in bone marrow supernatant, tyrosine and tryptophan biosynthesis pathways.

Conclusions: Our results show that Citrobacter infection may be a driving factor for aplastic anaemia, identifying a potential role for stearic acid in the immunopathogenesis of aplastic anaemia. Our study also demonstrates the potential role of 22-carbon long-chain polyunsaturated fatty acids, which may not only be involved in the metabolism of fibroblasts in bone marrow but also influence the formation of the bone marrow microenvironment, in aplastic anaemia.

Background

Aplastic anaemia is a severe form of anaemia caused by bone marrow failure and is often associated with lipomatosis of the bone marrow. Almost all cases of acquired regenerative anaemia appear to be mediated by immunity [1]. The immunopathogenesis of aplastic anaemia has long been a hot topic in the field of the disease, but metabolic studies in patients with aplastic anaemia are rare. Previous studies, however, have shown that myelolipemia, a common condition in patients with aplastic anaemia, involves a variety of metabolites, especially fatty acids. Myelolipemia has been identified as a competitive process between bone marrow adipocytes and osteoblasts derived from a common mesenchymal stem cell; this process involves the Wnt/β-catenin signalling pathway [2], Wnt signalling pathway inhibitor DKK1 [3], antagonist-associated secretory protein SFRP1 (Bodine et al., 2004), and paracrine and hormonal signalling pathways. Omega-3 unsaturated fatty acids and palmitic acid inhibit the differentiation of fibroblasts into osteoblasts by regulating these signalling pathways [4]. Saturated fatty acids produced by bone marrow adipocytes have a positive feedback effect on bone marrow adipogenesis by inhibiting osteoblast function and promoting adipocyte synthesis [5]. Palmitic acid can reduce the expression of RANKL, DKK1 and sclerosing protein in osteocytes and induce the apoptosis of osteoblasts, thus reducing the survival rate of bone cells [6]. Thus, we hypothesize that fatty acid metabolism and the process of bone marrow steatosis derived from AA are inextricably linked. What is not clear, however, is the change in fatty acid metabolism in aplastic anaemia patients. The correlation between intestinal microflora and lipid metabolism has been increasingly recognized. First, gut microbes are involved in short-chain fatty acid production and metabolism [7]. In the intestine, *Akkermansia muciniphila* metabolizes propionic acid [8]. *Bacteroides vulgatus* and *Bacteroides thetaiotaomicron* produce propionate through the succinate pathway. The main source of butyrate is in the clostridial clusters of obligate anaerobes, a small fraction of which produce propionate via the lactate pathway[9]. In addition to the SCFA regulation of intestinal homeostasis, gut-derived SCFAs can also affect parenteral tissues and organs through blood circulation [10]. SCFAs affect the immune response by regulating the activity of histone deacetylases in the immune cell genome and by regulating signalling through G protein-coupled receptors in immune cells[11,12]. In our previous study, we found a significant difference between the microbiome in patients with aplastic anaemia and that in normal controls. The abundances of Enterobacteriaceae and lactobacilli in the AA group were higher than those in the NC group, but the abundances of Bacteroides, Clostridium and Erysipelas were lower. At the species level, there are higher abundances of E. coli and *Clostridium citroniae* but lower abundances of *Prevotella copri*, *Roseburia faecis*, and *Ruminococcus bromii*[7]. Therefore, fatty acid levels in bone marrow supernatants and peripheral plasma were measured in patients with aplastic anaemia syndrome and normal controls. The differences in the levels of microorganisms, metabolic pathways and metabolites between the two groups were analysed by metagenomic sequencing. The aim of this study was to elucidate the changes in fatty acid metabolism in patients with aplastic anaemia and to determine how they might be related to gut microbes.

Materials And Methods

Patients

Twelve patients aged 15 to 81 years, with a median age of 46 years, were newly diagnosed with aplastic anaemia at the Tianjin Medical University General Hospital between September 2020 and June 2020 (AA group). Bone marrow supernatant, peripheral blood plasma and stool samples were collected before

treatment. The admission criteria were as follows: patients who did not take antibiotics, probiotics or other haematologic diseases within 3 months prior to admission. Bone marrow supernatant, peripheral blood plasma and stool samples were also collected from ten healthy volunteers. This study was approved by the Ethics Committee of Tianjin Medical University General Hospital, and informed written consent was obtained from all patients or their parents according to the Declaration of Helsinki.

Instruments and reagents

The following instruments and reagents were used: a - 80 °C refrigerator (Haier), a sterile EPPENDORF tube (Tianjin Haoyang Biotechnology Co., Ltd.), a Thermo Trace 1310-ISQ LT gas-mass spectrometer (Thermo), a refrigeration centrifuge (Hunan Instrument, H1850R), an electrothermal thermostatic water bath (Chang'an scientific instrument), a Covaris M220 ultrasound instrument (Covaris, Woburn, MA, USA), an NEBNext TM DNA Kit for Illumina (NEB, USA), a fluorescence quantizer (Qubit fluorometer, USA), and an Illumina NOVASE6000PE150. Phosphoric acid (Chinese medicine), ether (Chinese medicine), acetic acid (Sigma ≥99.5%), propionic acid (Sigma > 99.0%), butyric acid (Sigma > 99.0%), isobutyric acid (Sigma > 99.0%), valeric acid (Sigma > 98.0%), isovaleric acid (Sigma > 99.0%), hexanoic acid (Aladdin ≥99.5%), isohexanoic acid (Sigma > 98%), n-hexane (Chinese medicine), chloroform (Vokai), water (Millipore), sulfuric acid (Chinese medicine), methanol (Chinese medicine), methyl salicylate (TCI ≥99%), 52 kinds of mixed fatty acid methyl esters, agarose (Chinese medicine). A QIAamp DNA Stool Mini Kit (Qiagen, Hilden, Germany), an Agencourt Ampure XP (Beckman, USA), and a GenNextTM NGS Library Quantification Kit.

DNA extraction

Total DNA was extracted from the faeces with a QIAamp DNA Stool Mini Kit (QIAGEN, Hilden, Germany). DNA completeness and purity were assessed by running the samples on 1.2% agarose gels. The concentration of DNA was determined on a Qubit fluorometer.

Metagenomic library preparation and sequencing

Extracted DNA was sheared with a Covaris M220 (Covaris, Woburn, MA, USA) programmed to generate 300-bp fragments. The sequencing libraries were constructed with a NEBNext® Ultra™ DNA Library Prep Kit for Illumina® (NEB, USA). The products were purified using AgarosAgencourt AMPure XP (Beckman, USA) and quantified using a GenNextTM NGS Library Quantification Kit (Toyobo, Japan). The libraries were sequenced using Illumina NovaSeq 6000 and 150-bp paired-end technology at TinyGen Bio-Tech (Shanghai) Co., Ltd.

Fatty acid sequencing

The contents of long-chain fatty acids, including acetic acid, alanic acid, isobic acid, butyric acid, isoprene, ethionic acid, and hexacids, in the bone marrow of the AA patients and NCs were measured. The medium/long-chain fatty acids examined included the following: ingric acid, niacin, xian acid, lauric acid, thirteen alkyd, nutmeg acid, anti-9-nutmeg oleic acid, shun-9-nutmeg, xenoacid acid, anti-10-15 oleic acid, shun-10-ten pentaenoleic acid, palmitic acid, anti-9-palm oleic acid, shun-9-palm oleic acid, hexane acid, anti-10-17oleic acid, shun-10-17oleic acid, stearic acid, trans rock celery acid, anti-oleic acid, anti-isoelic acid, rock celeric acid, oleic acid, isooleic acid, anti-linoleic acid, anti-7-19 carbonic acid, anti-10-19 carbonic acid, linoleic acid, peanut acid, γ-linoleic acid, anti-11-20 carbonic acid, shun-20 11-20 carbonic acid, α-linoleic acid, 21 alkane acid, shun-11, 14-20 carbon dioleic acid, yamic acid, HOMO-γ-linoleic acid, bajuic acid, mustard acid, shun-11, 14, 17-20 carbon trioleic acid, peanut tetraoleic acid, 23 alkane acid, shun-13, 16-22 carbon dioleic acid, EPA, wood wax acid, nerve acid, shun-7, 10, 13, 16-22 carbon tetraoleic acid, DPA, DPA, and DHA.

Standard configuration

The short-chain fatty acids examined were as follows: acetic acid, propylene acid, butyric acid, isobic acid, ethyl acid, isoprene, and hexacid. Pure standard products were mixed with ether to make nine standard concentration gradients (0.02 sg/mL, 0.1 sg/mL, 1 sg/mL, 2 sg/mL, 5 sg/mL，10 μg/mL，25 μg/mL，50 μg/mL，and 100 μg/mL). Both the stock solution and the standard solution were stored at 0 °C.

The medium/long chain fatty acids were synthesized as follows: 52 fatty acid methyl ester solutions were mixed with positive hexane to make 10 standard concentration gradients (1 sg/mL, 5 sg/mL, 10 sg/mL, 25 sg/mL, 50 sg/mL, 100 μg/mL, 250 μg/mL, 500 μg/mL, 1000 μg/mL, and 2000 μg/mL). The concentration is the total concentration of each component (51 standard fatty acid methyl esters). The stock solution was stored at -80 °C and is now available as a standard solution.

Sample pretreatment

The short-chain fatty acids were synthesized as follows: the sample was transferred to a 2 mL centrifuge tube; 50 μL of 15 % phosphoric acid, 10 μL of 75 μg/mL of the internal label (iso-acid) solution and 140 μL of ether were added; the mixture was subjected to vortex oscillation for 1 min and centrifugation for 10 min at 4 °C (12000 rpm) for liquidation detection.

The medium/long-chain fatty acids were synthesized as follows: the appropriate amount of sample was transferred to a 15 mL centrifuge tube; 2 mL 1% methanol sulfate solution was added and mixed for 1 min; the mixture was esterified for 30 min in a water bath at 80 °C; the solution was removed and cooled; 1 mL positive hexane extraction was added, the mixture was washed with 5 mL H_2O (4 °C), centrifuged at 12000 rpm at 4 °C for 10 min, placed in an oscillating mixer for 30 s, centrifuged at 12000 rpm for 5 min, and subjected to precise absorption of 300 sL of upper liquid in a 2 mL centrifuge tube; 15 sl 500 ppm salicylic acid was added as the internal label; and the mixture was placed in an oscillating mixer for 10 sand subjected to precise absorption of 250 sL (added to the test bottle).

GC–MS detection

The chromatographic conditions were as follows: an Agilent HP-INNOWAX capillary column (30 m x 0.25 mm ID x 0.25 μm) was used; the inlet temperature was 250 °C, the ion source temperature was 230 °C, and the transmission line temperature was 250 °C for the four poles; the bar temperature was 150 °C. The program began at a starting temperature of 90 °C, was increased to 120 °C, was increased to 150 °C at a rate of 5 °C/min, and then was increased to 250 °C at a rate of 25 °C/min. The helium carrier had a carrier flow rate of 1.0 mL/min. MS conditions were as follows: electron blast ionization (EI) source, SIM scan mode, and electron energy: 70 eV.

Data analysis:

The raw fastq files were demultiplexed based on the index. The raw, paired-end reads were trimmed and quality controlled using Trimmomatic (http://www.usadellab.org/cms/?page=trimmomatic) and cutadapt software. The host sequences were removed by using BWA (http://biobwa.sourceforge.net/). The reformatted data were assembled and predicted by Megahit (https://github.com/voutcn/megahit) and METAProdigal (http://prodigal.ornl.gov/) software. The predicted genes were clustered, and a nonredundant gene catalogue was constructed with the CD-HIT package (http://www.bioinformatics.org/cd-hit/) (parameters: identity=95%, coverage=90%). The abundance of genes was quickly estimated by genomeCoverageBed in bedtools. The representative sequences were assigned for taxonomy against the NR database with an e-value of 1e-5 by DIAMOND software. The taxonomic information included the domain, kingdom, phylum, class, order, family, genus, and species. To understand the functions of the differentially expressed genes, the genes were assigned against the eggNOG database, KEGG database, GO database, CAZy database and ARDB database by using BLASTP (BLAST Version 2.2.28+, http://blast.ncbi.nlm.nih.gov/Blast.cgi) with an e-value of 1e-5.

For the bar graphs, VENN, heatmap analysis, PCA, PCoA, and NMDS were used, and the results were plotted with R (Version 3.4.1). Corr. R language (psych package) was used to determine the abundances of the differential expressed fatty acids and genes. Spearman correlation analysis was carried out by the test function, and visualization was carried out by the pheatmap package.

Results

Bone marrow fatty acid metabolism in patients with aplastic anaemia:

Changes in supernatant fatty acids in the bone marrow of patients with aplastic anaemia:

Orthogonal least squares discriminant analysis (OPLS-DA) were used to analyse the major fatty acids in the AA and NC groups (Tab 1,Fig 1). In the bone marrow supernatant, there was a significant difference in the short-chain fatty acid compositions, while there were no significant differences in the medium- and long-chain fatty acid compositions. There were significant differences in 3 of the 7 short-chain fatty acids tested. Among the 52 types of medium- and long-chain fatty acids detected, only one showed a significant difference. The major difference between patients with aplastic anaemia and normal controls was short-chain fatty acid metabolism.

Tab 1:OPLS-DA analysis

	pre	R2X(cum)	R2Y(cum)	Q2(cum)
AABM vsNCBM□C6-C24FA□	2	0.543	0.614	0.272
AABM vs NCBM□C1-C6FA□	1+4+0	0.965	0.881	0.732

Compared to the NC group, the contents of docosatetraenoate (C22:4) ($p < 0.05$) were significantly decreased, and the contents of isovaleric acid ($p < 0.001$), isobutyric acid ($p < 0.0001$) and valeric acid ($p < 0.005$) were significantly increased (Tab 2, Fig 2).

Tab 2 .Changed fatty acids in the bone marrow

	mean_AABM	sd_AABM	mean_NCBM	sd_NCBM	Fold Change_AABM/NCBM	log2(FC_AABM/NCBM)	p.value
C22:4	3.290286	0.954465	4.503714	1.01609	0.73057	-0.4529	0.011129
Isobutyric acid	0.03425	0.014858	0.0124	0.005125	2.7621	1.4658	9.79E-05
Isovaleric acid	0.030167	0.01777	0.0159	0.002726	1.8973	0.92393	0.000159
Valeric acid	0.025583	0.011033	0.0141	0.002767	1.8144	0.85951	0.002924
Acetic acid	2.572667	0.974088	1.5007	0.520259	1.7143	0.77763	0.005073

Changes in plasma fatty acids in patients with aplastic anaemia:

OPLS-DA were used to analyse the major fatty acids in the AA and NC groups (Tab 3 and Figs 3). In the peripheral plasma, there were significant differences in medium- and long-chain fatty acid compositions, while there were no significant differences in short-chain fatty acid copositions. Among the 52 types of

medium- and long-chain fatty acids detected, there were significant differences in the contents of 16. Only one of the seven short-chain fatty acids evaluated showed a significant difference. The major difference between aplastic anaemia patients and normal controls is short-chain fatty acid metabolism.

Tab 3 the OPLS-DA analysis of fatty acids in plasma

	pre	R2X(cum)	R2Y(cum)	Q2(cum)
AAPB vs NCPB（C6-C24FA）	3	0.74	0.837	0.535
AAPB vs NCPB（C1-C6FA）	1+2+0	0.935	0.357	0.276

Compared to the NC group, in the AA group, the contents of myristelaidate (C14:1T) ($p < 0.001$) and isobutyric acid ($p < 0.05$) were increased significantly. The medium and long-chain fatty acids with significant reductions were Caproate (C6:0)（P<0.01）, palmitelaidate (C16:1T)（P（0.001）, 10-heptadecenoate (C17:1)（P<0.01）, 10-transsheptadecenoate (C17:1T)（P<0.05）, stearate (C18:0)（P<0.01）, petroselaidate (C18:1N12T)（P<0.01）, transvaccenate (C18:2N7T) （P<0.05）, linoelaidate (C18:2N6T)（P<0.05）, 7-transnonadecenoate (C19:1N12T)（P<0.001）, eicosenoate (C20:1)（P<0.05）, trans 11-eicosenoate (C20:1T) （P<0.01）, erucate (C22:1N9)（P<0.05）, brassidate (C22:1N9T)（P<0.05）, docosadienoate (C22:2)（P<0.05）, docosatetraenoate (C22:4)（P<0.05）, and nervonoate（C24:1）（P<0.01）(Tab 4, Fig 4).

Tab 4 changed fatty acids(including long-chain fatty acids and short-chain fatty acids) in AA group in plasm.

	mean_AAB	sd_AAB	mean_NCB	sd_NCB	Fold Change_AAB/NCB	log2(FC_AAB/NCB)	p.value
C14:1T	20.41007	6.087152	14.15148	2.00612	1.4423	0.52833	0.000869
C19:1N12T	4.507297	0.7233	6.090836	0.770336	0.74001	-0.43438	0.000869
C16:1T	2.730239	0.552947	3.7321	0.519632	0.73156	-0.45096	0.001736
C17:1	3.526343	0.774811	4.735835	1.068266	0.74461	-0.42545	0.006211
C24:1	3.344069	0.897316	4.843347	1.091746	0.69045	-0.5344	0.006211
C18:0	405.9224	57.07996	481.828	62.47371	0.84246	-0.24731	0.009199
C18:1N12T	1.851153	0.43985	2.313218	0.34065	0.80025	-0.32148	0.009199
C20:1T	3.401346	0.501943	4.125306	0.597002	0.82451	-0.2784	0.009199
C17:1T	4.212472	0.721826	5.238189	0.767364	0.80418	-0.3144	0.011129
C20:1	4.555985	0.75348	5.501479	0.752388	0.82814	-0.27206	0.011129
C6:0	0.441762	0.28031	0.615143	0.140688	0.71814	-0.47765	0.013306
C22:1N9T	3.958385	0.607051	4.667704	0.664834	0.84804	-0.2378	0.022914
C22:1N9	7.894534	1.210693	9.309187	1.325933	0.84804	-0.2378	0.022914
C22:2	0.969069	0.331208	1.325357	0.314959	0.73118	-0.45171	0.022914
C22:4	2.972657	1.104194	3.86212	1.149583	0.7697	-0.37764	0.022914
C18:2N6T	1.0497	0.258317	1.28606	0.226167	0.81621	-0.29298	0.02718
C18:1N7T	7.464862	1.388793	8.935318	1.527666	0.83543	-0.2594	0.037797
Isobutyric acid	0.039	0.053662	0.0136	0.01152	2.8676	1.5199	0.034652

Faecal microbe changes in patients with aplastic anaemia:

Metagenomic sequencing showed that the microbial abundance in the faecal microflora of the AA group was changed at six levels: phylum, class, order, family, genus and species.

Species abundance changes in the AA group

β diversity analysis showed no significant difference in microbial abundance between the AA and NC groups, but the tendency of grouping is obvious.(Fig 5).

Phylum level: According to the α diversity analysis, there was no difference in coverage, sobs, or the Chao, ACE or Simpson index between the AA and NC groups, but the difference in the Shannon index, which was a parameter of colony diversity, was significant ($p = 0.010$)(Fig 6). The analysis of group differences confirmed that the overall microbial abundances of bacteria and eukaryotes at the phylum level were decreased in the AA group. The microbial abundances of Candidatus_ Zambryskibacteria, Candidatus_ Falkowbacteria, Candidatus_ Yanofskybacteria and Nematoda were increased in the AA group (Tab 5, Fig 7).

Tab 5. .the specific changed ID in the phylum level

level	.ID	p.value	p.signif	method	mean(AA)	n(AA)	mean(NC)	n(NC)
B	p__	0.005645	**	Wilcoxon	5326.235	12	8399.529	10
B	p__Candidatus_Falkowbacteria	0.043118	*	Wilcoxon	8.560287	12	1.824681	10
B	p__Candidatus_Yanofskybacteria	0.035419	*	Wilcoxon	0.015688	12	9.207157	10
B	p__Candidatus_Zambryskibacteria	0.019208	*	Wilcoxon	0.418214	12	0.118341	10
E	p__	0.011153	*	Wilcoxon	7.880836	12	1275.989	10
E	p__Nematoda	0.04257	*	Wilcoxon	223.77	12	327.3807	10

Class level：In the AA group, there were no significant differences in α diversity (Fig 8). The results showed no significant changes in the sequencing depth, species quantity, distribution uniformity, colony abundance, diversity, or microbial diversity in the AA group. The differential analysis showed that the abundances of Sphingobacteriia (bacteria), Oomycetes and Enoplea (eukaryotes) were decreased in the AA group (Tab 6, Fig 9).

Tab 6.the specific changed ID in the class level

level	.ID	p.value	p.signif	method	mean(AA)	n(AA)	mean(NC)	n(NC)
B	c__Sphingobacteriia	0.029961	*	Wilcoxon	56.00991	12	140.242	10
E	c__Oomycetes	0.008957	**	Wilcoxon	0.659821	12	6.989042	10
E	c__Enoplea	0.04257	*	Wilcoxon	217.3663	12	326.564	10

Order level: The same α diversity analysis showed no significant difference between the two groups(Fig 10). Specific difference analysis revealed decreased abundances of the bacterial orders Burkholderiales, Enterobacterales and Sphingobacteriales and the eukaryotic orders Peronosporales and Trichinellida in the AA group (Tab 7, Fig 11).

Tab 7. the specific changed ID in the order level

level	.ID	p.value	p.signif	method	mean(AA)	n(AA)	mean(NC)	n(NC)
B	o__Burkholderiales	0.029961	*	Wilcoxon	798.2971	12	3142.975	10
B	o__Rhodobacterales	0.035828	*	Wilcoxon	23.62861	12	43.59014	10
B	o__Sphingobacteriales	0.029961	*	Wilcoxon	55.21925	12	140.2076	10
E	o__Peronosporales	0.008957	**	Wilcoxon	0.659336	12	6.850161	10
E	o__Trichinellida	0.04257	*	Wilcoxon	217.3663	12	326.564	10

Family level: At the family level, the α diversity analysis also showed no significant difference between the two (Fig 12). The microbial abundances of Peronosporaceae, the Trichuridae family, alcaligenaceae in the eukaryotic kingdom, Rhodobacteraceae, Ruminococcaceae, Sphingobacteriaceae and Yersiniaceae family in the bacterial kingdom were decreased in the AA group. The microbial abundance of the Enterocytozoonidae family of the eukaryotic kingdom was elevated in the AA group (Tab 8, Fig 13).

Tab 8. the specific changed ID in the family level

level	.ID	p.value	p.signif	method	mean(AA)	n(AA)	mean(NC)	n(NC)
B	f__Alcaligenaceae	0.0169	*	Wilcoxon	15.96707	12	22.477	10
B	f__Rhodobacteraceae	0.035828	*	Wilcoxon	23.18635	12	42.36301	10
B	f__Ruminococcaceae	0.02058	*	Wilcoxon	113635.9	12	47871.68	10
B	f__Sphingobacteriaceae	0.02058	*	Wilcoxon	53.83421	12	131.7942	10
B	f__Yersiniaceae	0.024916	*	Wilcoxon	120.5516	12	153.3019	10
E	f__Peronosporaceae	0.008957	**	Wilcoxon	0.659336	12	6.850161	10
E	f__Enterocytozoonidae	0.015062	*	Wilcoxon	0.964247	12	0.124079	10
E	f__Trichuridae	0.04257	*	Wilcoxon	217.3663	12	326.564	10

Genus level: There was no significant difference in α diversity at the genus level(Fig 14). In eukaryotes, however, the abundances of Arabidopsis, Cucurbita and Enterocytozoon, as well as Cruoricaptor, Absiella, Afifella, Desulfobacca, Desulfosarcina, Dokdonia, Drancourtella, Enhydrobacter, Helicobacter, Lentzea, Rhodoferax, Smithella, Subdoligranulum, and Thiomargarita in the bacterial kingdom, were increased in the AA group. The abundances of Lambdavirus, Rtpvirus, Achromobacter, Burkholderia, Mycoavidus, Thiomonas, Caecibacter, Catenibacterium, Chloroherpeton, Citrobacter, Desulfatirhabdium, Friedmanniella, Haematomicrobium, Megasphaera, Oceanicaulis, Petrimonas, Serratia, Sneathia, Treptobacillus, Succinispira, and Sulfuricurvum in the bacterial kingdom showed the opposite trend (Tab 9, Fig 15).

Tab 9. the specific changed ID in the genus level

level	.ID	p.value	p.signif	method	mean(AA)	n(AA)	mean(NC)	n(NC)
B	g__Achromobacter	0.007145	**	Wilcoxon	10.09373	12	12.26749	10
B	g__Burkholderia	0.003436	**	Wilcoxon	14.80387	12	31.55629	10
B	g__Cruoricaptor	0.008635	**	Wilcoxon	103.0674	12	0.00011	10
B	g__Mycoavidus	0.005645	**	Wilcoxon	0.850142	12	5.981828	10
B	g__Thiomonas	0.008957	**	Wilcoxon	8.839875	12	26.5866	10
B	g__Absiella	0.029961	*	Wilcoxon	205.4508	12	89.55985	10
B	g__Afifella	0.027812	*	Wilcoxon	0.100013	12	0	10
B	g__Caecibacter	0.015976	*	Wilcoxon	0.729265	12	15.54945	10
B	g__Catenibacterium	0.02058	*	Wilcoxon	305.7946	12	2616.767	10
B	g__Chloroherpeton	0.028942	*	Wilcoxon	0.004109	12	0.128666	10
B	g__Citrobacter	0.04257	*	Wilcoxon	736.4254	12	2760.517	10
B	g__Desulfatirhabdium	0.02215	*	Wilcoxon	0.157288	12	0.743299	10
B	g__Desulfobacca	0.013201	*	Wilcoxon	0.065557	12	0	10
B	g__Desulfosarcina	0.029085	*	Wilcoxon	0.209741	12	0.168518	10
B	g__Dokdonia	0.035916	*	Wilcoxon	0.552809	12	0.037748	10
B	g__Drancourtella	0.024916	*	Wilcoxon	499.5553	12	131.7744	10
B	g__Enhydrobacter	0.018256	*	Wilcoxon	0.629597	12	0.045162	10
B	g__Friedmanniella	0.035706	*	Wilcoxon	0.019968	12	0.512966	10
B	g__Haematomicrobium	0.018657	*	Wilcoxon	0.010867	12	0.541071	10
B	g__Helicobacter	0.04257	*	Wilcoxon	119.9702	12	50.31599	10
B	g__Lentzea	0.029085	*	Wilcoxon	0.151672	12	0.007282	10
B	g__Megasphaera	0.0169	*	Wilcoxon	120.5764	12	5919.09	10
B	g__Oceanicaulis	0.021299	*	Wilcoxon	0	12	1.017431	10
B	g__Petrimonas	0.032066	*	Wilcoxon	1.570891	12	15.53802	10
B	g__Rhodoferax	0.042226	*	Wilcoxon	0.437173	12	0.068321	10
B	g__Serratia	0.0169	*	Wilcoxon	93.35629	12	116.9199	10
B	g__Smithella	0.035001	*	Wilcoxon	1.334781	12	0.008958	10
B	g__Sneathia	0.026317	*	Wilcoxon	0.0823	12	2.193245	10
B	g__Streptobacillus	0.035828	*	Wilcoxon	4.371066	12	9.960238	10
B	g__Subdoligranulum	0.035828	*	Wilcoxon	6958.998	12	2711.458	10
B	g__Succinispira	0.011106	*	Wilcoxon	0.329153	12	1.923889	10
B	g__Sulfuricurvum	0.024787	*	Wilcoxon	0.163208	12	0.507412	10
B	g__Thiomargarita	0.01856	*	Wilcoxon	5.323346	12	0.009884	10
B	s__Armatimonadetes_bacterium_CG_4_8_14_3_um_filter_66_20	0.027812	*	Wilcoxon	0.068908	12	0	10
E	g__Arabidopsis	0.034593	*	Wilcoxon	0.131755	12	0.006128	10
E	g__Cucurbita	0.027812	*	Wilcoxon	0.037481	12	0	10
E	g__Enterocytozoon	0.015062	*	Wilcoxon	0.964247	12	0.124079	10
E	g__Plasmopara	0.01377	*	Wilcoxon	0.629125	12	6.22372	10
E	g__Trichuris	0.04257	*	Wilcoxon	217.3663	12	326.564	10
V	g__Lambdavirus	0.006674	**	Wilcoxon	0.13463	12	2.01234	10
V	g__Rtpvirus	0.008557	**	Wilcoxon	0.001132	12	912.9737	10

Species level: Similarly, there were no significant differences observed in the α diversity analysis at the species level(Fig 16). However, in the AA group, the abundances of 84 species were increased, including 2 species in the viral kingdom (Staphylococcus_phage_phiSA_BS2, Streptococcus_phage_P0092), 2 species in the eukaryotic kingdom (Candida_maltosa, Enterocytozoon_bieneusi), 2 species in the archaea kingdom (Methanobacterium_congolense, Methanosarcina_spelaei) and 78 species in the bacterial kingdom (Proteus species, Clostridioides species, Ruminococcus species, etc.). A total of 125 microbial species were downregulated in the AA group, including 6 species in the viral kingdom（Stx1-converting_phage_phi-O153 , Enterococcus_phage_EFDG1 , Enterococcus_phage_EFLK1 , Escherichia_phage_vB_Ecos_CEB_EC3a, Escherichia_virus_186, Streptococcus_virus_ALQ132）, 1 species in the eukaryotic kingdom (Plasmopara_halstedi)；2 species in the archaea kingdom（Candidatus_Altiarchaeales_archaeon_WOR_SM1_79, Methanosphaera_sp._rholeuAM270 ） and 116 species in the bacterial kingdom（Prevotella_sp._CAG:386, Bifidobacterium_dentium, [Eubacterium]_eligens, Clostridium_sp._CAG:7, Catenibacterium_mitsuokai, etc(Tab 10,Fig 17).

Tab 10. the specific changed IDs in the species level(only shows the top 20 species ID)

.ID	p.value	p.signif	method	mean(AA)	n(AA)	mean(NC)	n(NC)
s__Subdoligranulum_sp._APC924/74	0.035828	*	Wilcoxon	4554.301	12	611.9317	10
s__Erysipelotrichaceae_bacterium_3_1_53	0.0169	*	Wilcoxon	3758.78	12	76.15913	10
s__Ruminococcus_sp.	0.04257	*	Wilcoxon	2141.948	12	97.13947	10
s__Bifidobacterium_dentium	0.04257	*	Wilcoxon	729.3444	12	6287.88	10
s__Catenibacterium_mitsuokai	0.0169	*	Wilcoxon	295.1914	12	1497.776	10
s__Ruminococcus_sp._DSM_100440	0.007145	**	Wilcoxon	281.9453	12	17.78605	10
s__Absiella_dolichum	0.029961	*	Wilcoxon	205.4508	12	89.55985	10
s__Drancourtella_massiliensis	0.029961	*	Wilcoxon	165.5897	12	11.95476	10
s__Clostridiales_bacterium_VE202-13	0.029961	*	Wilcoxon	160.2015	12	31.45474	10
s__Bifidobacterium_sp._MSTE12	0.02058	*	Wilcoxon	106.8885	12	881.9638	10
s__Cruoricaptor_ignavus	0.008635	**	Wilcoxon	103.0674	12	0.00011	10
s__Sulfurospirillum_halorespirans	0.015853	*	Wilcoxon	95.34377	12	0.006698	10
s__Clostridium_acetireducens	0.04257	*	Wilcoxon	86.51676	12	38.70515	10
s__Fusobacterium_sp._CM21	0.02058	*	Wilcoxon	68.64265	12	25.16005	10
s__Bifidobacterium_saeculare	0.02058	*	Wilcoxon	65.66262	12	16.88376	10
s__Curvibacter_putative_symbiont_of_Hydra_magnipapillata	0.035828	*	Wilcoxon	57.01436	12	9.584941	10
s__uncultured_actinobacterium_HF0500_35G12	0.003436	**	Wilcoxon	14.16386	12	2.742277	10
s__Citrobacter_werkmanii	0.024916	*	Wilcoxon	14.11588	12	118.4372	10
s__Enterococcus_saccharolyticus	0.037581	*	Wilcoxon	11.35573	12	0.137005	10
s__uncultured_alpha_proteobacterium_HF0070_14E07	0.029961	*	Wilcoxon	10.1125	12	20.48859	10

Changes in the KEGG signalling pathway in the AA group

Compared with the normal control group, there were significant differences in the abundances of genes involved in 12 signalling pathways in the AA group. Among them, the abundances of genes involved in 2 metabolism-related pathways were upregulated (penicillin and cephalosporin biosynthesis and tyrosine and tryptophan biosynthesis). In addition, the abundances of genes involved in eight metabolism-related pathways, including nonribosomal peptides, betalain biosynthesis, and lysine degradation, showed the opposite trend. We also observed the downregulation of genes involved in pathways related to type I diabetes mellitus in humans (Fig 18, Tab 11).

Tab 11.Changed abundance of specific KEGG pathway ID in AA group

.ID	p.value	p.format	p.signif	method	mean(AA)	n(AA)	mean(NC)	n(NC)
Betalain biosynthesis	0.035828	0.036	*	Wilcoxon	23.44387	12	30.77787	10
Biosynthesis of siderophore group nonribosomal peptides	0.024916	0.025	*	Wilcoxon	202.6813	12	394.1924	10
Caprolactam degradation	0.035828	0.036	*	Wilcoxon	61.81826	12	90.93364	10
Drug metabolism - cytochrome P450	0.04257	0.043	*	Wilcoxon	148.2111	12	213.5611	10
Lysine degradation	0.029961	0.030	*	Wilcoxon	701.4266	12	923.5934	10
Metabolism of xenobiotics by cytochrome P450	0.04257	0.043	*	Wilcoxon	148.3814	12	215.1718	10
N-Glycan biosynthesis	0.035828	0.036	*	Wilcoxon	63.28539	12	95.42845	10
Penicillin and cephalosporin biosynthesis	0.0169	0.017	*	Wilcoxon	197.2371	12	136.6711	10
Phenylalanine, tyrosine and tryptophan biosynthesis	0.04257	0.043	*	Wilcoxon	4709.729	12	4261.92	10
Type I diabetes mellitus	0.029961	0.030	*	Wilcoxon	371.8122	12	426.242	10
Ubiquinone and other terpenoid-quinone biosynthesis	0.035828	0.036	*	Wilcoxon	978.2562	12	1304.532	10
Valine, leucine and isoleucine degradation	0.011153	0.011	*	Wilcoxon	1148.773	12	1354.179	10

Changes in fatty acid levels in the AA group were associated with microbial species

Correlation between fatty acid content in the bone marrow supernatant and faecal microbial abundance

The abundance of the uncultured_ actinobacterium_ HF0500_ 35g12 species in the bacterial kingdom was positively correlated with the valeric acid content, which is negatively correlated with the microbial abundances of the Candidatus_ Zambryskibacteria phylum, the genus Cruoricaptor, the *Cruoricaptor_ ignavus* species, the genus drancourtella, the Bifidobacterium_ Saeculare species, the Drancourtella_ Massiliensis species, the Pseudomonas_ Syringae species, the Sulfurospirillum_ Halorespirans species and the Staphylococcus_phage_phiSA_BS2 species in the viral kingdom. There as a positive correlation between isobutyric acid and the microbial abundances of the Sphingobacteriia class, Sphingobacteriales order, Sphingobacteriaceae family, Afifella genus , and Enterococcus_sp._4E1_DIV0656 species. The abundance of microbes in the bacterial kingdom that showed a negative correlation with the isobutyrate content included those in the Absiella genus, Absiella_dolichum species, Cruoricaptor genus, Cruoricaptor_ignavus species , Mycoavidus genus , Mycoavidus_cysteinexigens species and 8 other microbial species. The abundance of Catenibacterium genus and Catenibacterium_mitsuokai speices in the bacterial kingdom was positively correlated with the content of Docosatetraenoate, which is negatively correlated with the microbial abundance of the Enhydrobacter genus, Enhydrobacter_aerosaccus species, Smithella genus, Bifidobacterium_sp._MSTE12 genus and 7 other species. The content of isovaleric acid showed a negative correlation with the abundances of the Drancourtella genus, Chloroflexi_bacterium_GWB2_49_20 species, Geobacillus_thermodenitrificans species, Kocuria_kristinae species, and Polaromonas_sp._JS666 species in the bacterial kingdom and the Methanobacterium_congolense species in archaea kingdom (Tab 12, Fig 19).

Tab 12.the specific correlation between the microbial abundance and fatty acids in the bone marrow supernatant in AA group(the species level showed in supplementary files)

nameA	nameB	correlation	P.value	method	star	group
B__c__Sphingobacteriia	Isobutyric.acid	0.677197	0.015554	spearman	*	AA
B__f__Sphingobacteriaceae	Isobutyric.acid	0.722811	0.007911	spearman	**	AA
B__g__Absiella	Isobutyric.acid	-0.61404	0.033666	spearman	*	AA
B__g__Afifella	Isobutyric.acid	0.626033	0.029428	spearman	*	AA
B__g__Cruoricaptor	Isobutyric.acid	-0.63042	0.027977	spearman	*	AA
B__g__Mycoavidus	Isobutyric.acid	-0.62106	0.031136	spearman	*	AA
B__o__Sphingobacteriales	Isobutyric.acid	0.722811	0.007911	spearman	**	AA
B__g__Drancourtella	Isovaleric.acid	-0.61378	0.033762	spearman	*	AA
B__g__Cruoricaptor	Valeric.acid	-0.65606	0.020517	spearman	*	AA
B__g__Drancourtella	Valeric.acid	-0.68652	0.013674	spearman	*	AA
B__p__Candidatus_Zambryskibacteria	Valeric.acid	-0.60596	0.036759	spearman	*	AA
B__g__Catenibacterium	C22:4	0.643357	0.024003	spearman	*	AA
B__g__Enhydrobacter	C22:4	-0.62678	0.029178	spearman	*	AA
B__g__Smithella	C22:4	-0.60184	0.038407	spearman	*	AA

Correlation between fatty acid content in the plasma and faecal microbial abundance

There were positive correlations between the abundances of the Citrobacter_rodentium species and Dysgonomonas_sp._BGC7 species in the bacterial kingdom and the content of stearate. The abundances of the Sphingobacteriia class, Sphingobacteriaceae order, Sphingobacteriales family, and Sphingobacterium_gobiense species were proportional to the contents of 10-heptadecenoate, petroselaidate, nervonoate and trans 11-eicosenoate. The abundances of the first three were also proportional to the contents of linoelaidate, and the latter was related to the contents of eicosenoate, rucate, brassidate and docosadienoate. There was a positive correlation between the abundances of the Catenibacterium genus, Catenibacterium_mitsuokai and Ralstonia_pickettii species and the content of docosatetraenoate. The abundance of Enterobacter_sp._50793107, Lactobacillus_equigenerosi, and Lactobacillus_pobuzihii species and the content of nervonoate showed the same correlation. The abundance of the Enterococcus_phage_EFDG1 species in the viral kingdom was also positively correlated with the contents of transvaccenate, linoelaidate, 7-transnonadecenoate and nervonoate.

In the AA group，there was a negative correlation between the abundance of microbes in the faeces and fatty acid content in the plasma, which showed a correlation between the abundances of the Desulfosarcina genus, Desulfosarcina_cetonica species, Succinispira genus, Succinispira_mobiliz species and 9 other species in the bacterial kingdom and the content of caproate. There was also a correlation between the content of docosadienoate and the abundances of the Enhydrobacter genus, Enhydrobacter_aerosaccus species, Mycoaviduss genus, Mycoavidus_cysteinexigens species and 5 other species in the bacterial kingdom. Therefore, there was a correlation between the content of isobutyric acid and the abundances of the Citrobacter genus, Citrobacter pasteurii species and Citrobacter sp. MGH106 species. The species abundances of Chloroflexi_ bacterium_ GWB2_ 49_ 20, Kocuria_ kristinae, and Lactobacillus_ Equigenerosi were negatively correlated with the content of petroselaidate, the latter two with the content of transvaccenate and the latter with the content of linoelaidate. The species abundances of Chloroflexi_bacterium_GWB2_49_20, Enterobacter_sp._50793107, Lactobacillus_equigenerosi, and Serratia_sp._TEL were negatively correlated with the contents of trans 11-eicosenoate, linoelaidate, brassidate, and erucate, the former 1 with the content of linoelaidate. There were also negative correlations between microbial abundance and the contents of various fatty acids, which showed a correlation between the abundance of the Lactobacillus_equigenerosi species and the contents of palmitelaidate, 10-heptadecenoate, 10-transsheptadecenoate, petroselaidate, transvaccenate, linoelaidate, 7-transnonadecenoate, eicosenoate, trans 11-eicosenoate, erucate, brassidate, docosadienoate, docosatetraenoate, nervonoate, and caproate. There was also a correlation between the abundances of the Cruoricaptor genus and Cruoricaptor_ignavus species and the contents of palmitelaidate, transsheptadecenoate, stearate, and caproate; a correlation between the abundance of the Lactobacillus_pobuzihii species the contents of 7-transnonadecenoate, nervonoate, and isobutyric acid; and a correlation between the abundance of Serratia_sp._TEL and the contents of 11-eicosenoate, trans 11-eicosenoate, erucate, brassidate, docosadienoate, and isobutyric acid. A negative correlation was also found between the species abundance of Enterobacter_sp._50793107 and the contents of trans 11-eicosenoate, erucate, brassidate, nervonoate and isobutyric acid. There was a negative correlation between the genus abundance of Lentzea and the contents of linoelaidate, 7-transnonadecenoate, and 11-eicosenoate; a negative correlation between the species abundance of Chloroflexi_bacterium_GWB2_49_20C and the contents of petroselaidate, linoelaidate, and 11-eicosenoate; a negative correlation between the species abundance of Bifidobacterium_saeculare and the contents of docosatetraenoate and caproate; a negative correlation between the species abundance of Gulbenkiania_indica and the contents of caproate and isobutyric acid; a negative correlation between the species abundance of Kocuria_kristinae and the contents of petroselaidate and transvaccenate; and a negative correlation between the species abundance of Xenorhabdus_innexi and the contents of docosadienoate and isobutyric acid. There was also a negative correlation between microbial abundance in the eukaryotic kingdom and fatty acid content in the plasma, which showed a negative correlation between the genus abundance of Arabidopsis and the content of 11-eicosenoate; and negative correlations between the species abundance of Candida_maltosa and the content of stearate， the genus abundance of Cucurbita and the contents of 10-heptadecenoate, petroselaidate, transvaccenate, linoelaidate, docosatetraenoate and the species

abundance of Cucurbita_moschata and the contents of 10-heptadecenoate, petroselaidate, transvaccenate, linoelaidate, and docosatetraenoate. The abundances of the Nematoda phylum, Enoplea class, Trichinellida order, Trichuridae family, and Trichuris genus were also negatively correlated with the contents of 11-eicosenoate and docosatetraenoate and the first was correlated with the content of transsheptadecenoate (Tab 13,.Fig 20).

Tab 13. the specific correlation between the microbial abundance and fatty acids in the plasma in AA group(only the top and last 20 showed here)

nameA	nameB	correlation	P.value	method	star	group
B__s__Dialister_invisus_CAG:218	C14:1T	0.839161	0.000643	spearman	**	AA
B__g__Catenibacterium	C22:4	0.797203	0.0019	spearman	**	AA
B__s__Catenibacterium_mitsuokai	C22:4	0.797203	0.0019	spearman	**	AA
B__s__Ralstonia_pickettii	C22:4	0.74081	0.005847	spearman	**	AA
B__s__Sphingobacterium_gobiense	C18:1N12T	0.739001	0.006033	spearman	**	AA
B__s__Lactobacillus_pobuzihii	C14:1T	0.734316	0.006538	spearman	**	AA
B__s__Citrobacter_rodentium	C18:0	0.734266	0.006543	spearman	**	AA
B__s__Sphingobacterium_gobiense	C20:1	0.727804	0.007291	spearman	**	AA
B__s__Cellulomonas_marina	C14:1T	0.681607	0.014642	spearman	*	AA
V__s__Enterococcus_phage_EFDG1	C18:2N6T	0.679284	0.015117	spearman	*	AA
V__s__Enterococcus_phage_EFDG1	C19:1N12T	0.668087	0.017569	spearman	*	AA
B__s__Dysgonomonas_sp._BGC7	C18:0	0.664336	0.018453	spearman	*	AA
B__s__Dialister_invisus	C14:1T	0.65035	0.022034	spearman	*	AA
B__s__Sphingobacterium_gobiense	C17:1T	0.645693	0.023332	spearman	*	AA
B__f__Sphingobacteriaceae	C17:1	0.636364	0.026097	spearman	*	AA
B__o__Sphingobacteriales	C17:1	0.636364	0.026097	spearman	*	AA
V__s__Enterococcus_phage_EFDG1	C18:1N7T	0.630764	0.027866	spearman	*	AA
B__c__Sphingobacteriia	C17:1	0.629371	0.02832	spearman	*	AA
B__f__Sphingobacteriaceae	C18:1N12T	0.629371	0.02832	spearman	*	AA
B__f__Sphingobacteriaceae	C20:1T	0.629371	0.02832	spearman	*	AA
E__f__Trichuridae	C22:4	-0.76224	0.00395	spearman	**	AA
E__g__Trichuris	C22:4	-0.76224	0.00395	spearman	**	AA
E__o__Trichinellida	C22:4	-0.76224	0.00395	spearman	**	AA
E__g__Cucurbita	C22:4	-0.7642	0.003803	spearman	**	AA
E__s__Cucurbita_moschata	C22:4	-0.7642	0.003803	spearman	**	AA
B__s__Serratia_sp._TEL	Isobutyric.acid	-0.77335	0.003173	spearman	**	AA
B__s__Paenibacillus_sp._Aloe-11	C6:0	-0.79499	0.010445	spearman	*	AA
B__s__Lactobacillus_equigenerosi	C17:1T	-0.79728	0.001897	spearman	**	AA
B__s__Enterococcus_durans	C6:0	-0.8	0.009628	spearman	**	AA
B__s__Enterobacter_ludwigii	Isobutyric.acid	-0.80911	0.001435	spearman	**	AA
B__s__Lactobacillus_equigenerosi	C18:2N6T	-0.83643	0.000696	spearman	**	AA
B__s__Lactobacillus_equigenerosi	C16:1T	-0.83999	0.000627	spearman	**	AA
B__s__Lactobacillus_equigenerosi	C18:1N12T	-0.83999	0.000627	spearman	**	AA
B__s__Lactobacillus_equigenerosi	C22:1N9	-0.83999	0.000627	spearman	**	AA
B__s__Lactobacillus_equigenerosi	C22:1N9T	-0.83999	0.000627	spearman	**	AA
B__s__Lactobacillus_equigenerosi	C22:2	-0.84355	0.000564	spearman	**	AA
B__s__Lactobacillus_equigenerosi	C24:1	-0.85423	0.000404	spearman	**	AA
B__s__Lactobacillus_equigenerosi	C20:1T	-0.85779	0.000359	spearman	**	AA
B__s__Myxococcus_stipitatus	C6:0	-0.87636	0.001935	spearman	**	AA
B__s__Vibrio_quintilis	C6:0	-0.87636	0.001935	spearman	**	AA

Changes in fatty acid levels in the AA group were correlated with the KEGG signalling pathway

There was a positive correlation between isovaleric acid, which was elevated in the bone marrow supernatant of individuals in the AA group, and the abundance of genes involved in the type I diabetes mellitus pathway. The lysine degradation pathway was positively correlated with the content of isobutyric acid, which was upregulated in both the peripheral plasma and bone marrow supernatant from the AA group but negatively correlated with stearate, which was downregulated in the peripheral plasma. The downregulated levels of docosadioate, 11-eicosenoate, stearate and docosatetraenoate in the peripheral plasma in the AA group were negatively associated with phenylalanine, tyrosine, and tryptophan biosynthesis, N-glycan biosynthesis, and betaine biosynthesis, respectively. The same correlation was also found between the content of docosadienoate and N-glycan biosynthesis (Tab 14, Fig 21).

Tab 14.the correlation between the abundance of KEGG pathway and fatty acids in plasma and bone marrow supernatant in AA group.

nameA	nameB	correlation	P.value	method	star	group
Betalain biosynthesis	C18:0	0.58042	0.047856	spearman	*	AABM
Lysine degradation	C18:0	0.608392	0.035806	spearman	*	AABM
N-Glycan biosynthesis	C20:1	0.643357	0.024003	spearman	*	AABM
N-Glycan biosynthesis	C22:2	0.678322	0.015317	spearman	*	AABM
Phenylalanine, tyrosine and tryptophan biosynthesis	C22:2	-0.58042	0.047856	spearman	*	AABM
Ubiquinone and other terpenoid-quinone biosynthesis	C22:4	0.622378	0.030676	spearman	*	AABM
Type I diabetes mellitus	Isovaleric.acid	0.61378	0.033762	spearman	*	AAPB
Lysine degradation	Isobutyric.acid	-0.57793	0.049049	spearman	*	AAPB

Correlations between microbial abundance alterations and KEGG signalling pathways in the AA group

The abundances of the Mycoavidus genus, Mycoavidus_cysteinexigens species, Achromobacter_sp._ATCC35328 species and Xenorhabdus_innexi species in the bacterial kingdom were negatively correlated with type I diabetes mellitus and positively correlated with the abundances of the Geobacillus_thermodenitrificans species and Kocuria_kristinae species in the bacterial kingdom and the abundance of the Methanobacterium_congolense species in the archaea kingdom. Ubiquinone and other terpenoid-quinone biosynthesis was positively correlated with the abundances of the Catenibacterium genus, Catenibacterium_mitsuokai and Ralstonia_pickettii species and negatively correlated with the abundances of the Desulfosarcina genus, Bifidobacterium_saeculare, Desulfosarcina_cetonica and Megasphaera_massiliensis species in the bacterial kingdom. The abundance of Planctomycetes_bacterium_TMED75 in the bacterial kingdom and Sphingobacterium_gobiense species was positively correlated with N-glycan biosynthesis, which was also negatively correlated with the abundances of Enhydrobacter, the Sulfuricurvum genus, Enhydrobacter_aerosaccus and 6 other species in the bacterial kingdom and the Nematoda phylum, Enoplea class, Trichinellida order, Trichurida family, Arabidopsis, and Trichuris genus in the eukaryotic kingdom. A positive correlation was also found between the abundances of Enhydrobacter and the Sulfuricurvum genera, Enhydrobacter aerosaccus, Enterobacter sp. CC120223-11 and 5 other species in the bacterial kingdom and the phenylalanine, tyrosine and tryptophan biosynthesis signalling pathways, as well as the abundances of the Citrobacter genus, Citrobacter_pasteurii, Citrobacter_rodentium, Citrobacter_sp._MGH106 and 3 other species in the bacterial kingdom and the lysine degradation signalling pathway. The correlation between the abundances of the Cucurbita genus and Cucurbita moschata species in eukaryotes and the phenylalanine, tyrosine and tryptophan biosynthesis signalling pathways was negative. A positive correlation was also found in the betalain biosynthesis signalling pathway and the abundances of the Citrobacter genus, Citrobacter_pasteurii, Citrobacter_rodentium, Citrobacter_sp._MGH106 and 4 other species (Tab 15,Fig 22).

Tab 15.the correlation between the microbial abundance and the KEGG pathway abundance.

nameA	nameB	correlation	P.value	method	star	level
B__g__Catenibacterium	Ubiquinone and other terpenoid-quinone biosynthesis	0.587413	0.044609	spearman	*	PB
B__s__Catenibacterium_mitsuokai	Ubiquinone and other terpenoid-quinone biosynthesis	0.587413	0.044609	spearman	*	PB
B__s__Ralstonia_pickettii	Ubiquinone and other terpenoid-quinone biosynthesis	0.592648	0.042283	spearman	*	PB
B__g__Desulfosarcina	Ubiquinone and other terpenoid-quinone biosynthesis	-0.73677	0.00627	spearman	**	PB
B__s__Bifidobacterium_saeculare	Ubiquinone and other terpenoid-quinone biosynthesis	-0.85315	0.000418	spearman	**	PB
B__g__Enhydrobacter	Phenylalanine, tyrosine and tryptophan biosynthesis	0.683116	0.014339	spearman	*	PB
B__s__Desulfosarcina_cetonica	Ubiquinone and other terpenoid-quinone biosynthesis	-0.84355	0.000564	spearman	**	PB
B__g__Sulfuricurvum	Phenylalanine, tyrosine and tryptophan biosynthesis	0.647234	0.022896	spearman	*	PB
B__s__Megasphaera_massiliensis	Ubiquinone and other terpenoid-quinone biosynthesis	-0.72727	0.007355	spearman	**	PB
B__s__Citrobacter_sp._MGH106	Phenylalanine, tyrosine and tryptophan biosynthesis	0.601399	0.038588	spearman	*	PB
B__s__Enhydrobacter_aerosaccus	Phenylalanine, tyrosine and tryptophan biosynthesis	0.683116	0.014339	spearman	*	PB
B__s__Enterobacter_sp._CC120223-11	Phenylalanine, tyrosine and tryptophan biosynthesis	0.65035	0.022034	spearman	*	PB
B__s__Lactobacillus_equigenerosi	Phenylalanine, tyrosine and tryptophan biosynthesis	0.597959	0.040012	spearman	*	PB
B__s__Oceanobacillus_oncorhynchi	Phenylalanine, tyrosine and tryptophan biosynthesis	0.717863	0.008563	spearman	**	PB
B__s__Streptomyces_scabiei	Phenylalanine, tyrosine and tryptophan biosynthesis	0.626434	0.029293	spearman	*	PB
B__s__uncultured_bacterium_5G12	Phenylalanine, tyrosine and tryptophan biosynthesis	0.643357	0.024003	spearman	*	PB
B__s__Planctomycetes_bacterium_TMED75	N-Glycan biosynthesis	0.70182	0.010957	spearman	*	PB
B__g__Enhydrobacter	N-Glycan biosynthesis	-0.73241	0.006752	spearman	**	PB
B__g__Sulfuricurvum	N-Glycan biosynthesis	-0.81099	0.00137	spearman	**	PB
B__s__Clostridium_sp._3-3	N-Glycan biosynthesis	-0.70629	0.010245	spearman	*	PB
B__s__Sphingobacterium_gobiense	N-Glycan biosynthesis	0.604638	0.037281	spearman	*	PB
B__g__Citrobacter	Lysine degradation	0.748252	0.005124	spearman	**	PB
B__s__Citrobacter_pasteurii	Lysine degradation	0.776224	0.002993	spearman	**	PB
B__s__Citrobacter_rodentium	Lysine degradation	0.594406	0.041521	spearman	*	PB
B__s__Citrobacter_sp._MGH106	Lysine degradation	0.769231	0.003446	spearman	**	PB
B__s__Enterobacter_ludwigii	Lysine degradation	0.881119	0.000153	spearman	**	PB
B__s__Enterobacter_sp._CC120223-11	Lysine degradation	0.79021	0.002223	spearman	**	PB
B__s__Enhydrobacter_aerosaccus	N-Glycan biosynthesis	-0.73241	0.006752	spearman	**	PB
B__s__Megasphaera_massiliensis	N-Glycan biosynthesis	-0.71329	0.009202	spearman	**	PB
B__s__Oceanobacillus_oncorhynchi	N-Glycan biosynthesis	-0.78312	0.002591	spearman	**	PB
B__s__uncultured_Citrobacter_sp.	Lysine degradation	0.748252	0.005124	spearman	**	PB
B__g__Citrobacter	Betalain biosynthesis	0.888112	0.000114	spearman	**	PB
B__s__Pontibacillus_litoralis	N-Glycan biosynthesis	-0.67182	0.016722	spearman	*	PB
B__s__Citrobacter_pasteurii	Betalain biosynthesis	0.818182	0.001143	spearman	**	PB
B__s__Citrobacter_rodentium	Betalain biosynthesis	0.839161	0.000643	spearman	**	PB

B__s__Citrobacter_sp._MGH106	Betalain biosynthesis	0.867133	0.00026	spearman	**	PB
B__s__uncultured_bacterium_5G12	N-Glycan biosynthesis	-0.71329	0.009202	spearman	**	PB
B__s__Enterobacter_ludwigii	Betalain biosynthesis	0.671329	0.016831	spearman	*	PB
B__s__Enterobacter_sp._CC120223-11	Betalain biosynthesis	0.776224	0.002993	spearman	**	PB
B__s__uncultured_Citrobacter_sp.	Betalain biosynthesis	0.839161	0.000643	spearman	**	PB
B__s__Yersinia_enterocolitica	Betalain biosynthesis	0.594406	0.041521	spearman	*	PB
E__c__Enoplea	N-Glycan biosynthesis	-0.6014	0.038588	spearman	*	PB
E__f__Trichuridae	N-Glycan biosynthesis	-0.6014	0.038588	spearman	*	PB
E__g__Arabidopsis	N-Glycan biosynthesis	-0.71288	0.009261	spearman	**	PB
E__g__Trichuris	N-Glycan biosynthesis	-0.6014	0.038588	spearman	*	PB
E__o__Trichinellida	N-Glycan biosynthesis	-0.6014	0.038588	spearman	*	PB
E__p__Nematoda	N-Glycan biosynthesis	-0.60839	0.035806	spearman	*	PB
E__g__Cucurbita	Lysine degradation	-0.57705	0.049477	spearman	*	PB
E__s__Cucurbita_moschata	Lysine degradation	-0.57705	0.049477	spearman	*	PB
A__s__Methanobacterium_congolense	Type I diabetes mellitus	-0.69406	0.012279	spearman	*	BM
B__g__Mycoavidus	Type I diabetes mellitus	0.58042	0.047856	spearman	*	BM
B__s__Achromobacter_sp._ATCC35328	Type I diabetes mellitus	0.587342	0.044641	spearman	*	BM
B__s__Geobacillus_thermodenitrificans	Type I diabetes mellitus	-0.7866	0.002405	spearman	**	BM
B__s__Kocuria_kristinae	Type I diabetes mellitus	-0.71596	0.008825	spearman	**	BM
B__s__Mycoavidus_cysteinexigens	Type I diabetes mellitus	0.58042	0.047856	spearman	*	BM
B__s__Xenorhabdus_innexi	Type I diabetes mellitus	0.585976	0.045263	spearman	*	BM

Discussion

Aplastic anaemia is defined as pancytopenia with hypocellular bone marrow in the absence of abnormal infiltrate and no increase in reticulin. To diagnose aplastic anaemia, there must be at least two of the following criteria: (i) haemoglobin <100 g/l, (ii) platelet count <50 × 10^9/l, and (iii) neutrophil count <1·5 × 10^9/l[13]. Most cases of aplastic anaemia are characterized as a bone marrow failure disorder caused by immune cells attacking their own haematopoietic stem cells, and the main effector cells identified are CD8+ T cells (also called cytotoxic T cells, CTLs) that express interferon γ [14]. However, the mechanism of CD8+ T cell activation is not clear. In addition to cytotoxic T cells, AA patients have immune disorders caused by a large number of other immune molecules. Th1 and Th2 cells are upregulated in aplastic anaemia patients, while Tregs (regulatory T cells) are downregulated in both quantity and function, triggering an autoimmune escape mechanism that drives disease progression [15,16]. The decrease in the number of Tregs may be due to infection-induced Th1 functional inhibition, which increases the inflammatory response and induces the functional impairment of Tregs [16]. Tregs can inhibit CD8+ T cell function by secreting inhibitory cytokines, inducing apoptosis and interacting with antigen-presenting cells [17]. Dendritic cells (DCs), a class of antigen-presenting cells, especially bone marrow-derived mDCs and plasma cell-derived pDCs. play a role in the pathology of aplastic anaemia. AA patients have upregulated numbers of DCs and high mDC/pDC ratios, as well as upregulated levels of mDC surface costimulatory molecules and pyruvate kinase 2 (PKM2), demonstrating an upregulation of mDC function [18-20]. Th17 cells are upregulated in the early disease course and positively correlate with the extent of disease activity, having an inverse relationship with the number of Treg cells, and upregulate Th1 cells by secreting IL-17 [21]. In addition, the pathogenesis of aplastic anaemia has been proven to be related to the bone marrow haematopoiesis microenvironment, in which AA patients contain fewer endosteal, vascular, and perivascular cells than healthy controls [22]. Moreover, MSCs from AA patients exhibit weaker proliferative capacity and modulate the bone marrow immune microenvironment by secreting multiple cytokines [23] while also having a stronger tendency to differentiate into adipocytes [24], which are increased in the haematopoietic microenvironment and lead to the inhibition of HSC differentiation and development [25]. In conclusion, aplastic anaemia is an immune disease with a complicated pathogenesis; however, the factors involved in the onset of aplastic anaemia are unclear. Our study revealed the role of lipid metabolism in the pathogenesis of aplastic anaemia through a large number of correlation analyses between macrogenes and lipid metabonomics and showed that *Citrobacter rodentium* may act as a motile factor in aplastic anaemia.

The species abundances of *Citrobacter pasteurii*, Citrobacter sp. MGH, and *Citrobacter rodentium* in the Citrobacter genus in the bacterial kingdom were downregulated in the AA group and had a positive correlation and negative correlation with the contents of stearate and isobutyric acid, respectively(Fig 23). While lysine degradation and the betalain biosynthesis pathway were positively correlated with Citrobacter species abundance, the former had a positive correlation and negative correlation with the contents of stearate and isobutyric acid in the plasma, respectively. Furthermore, the isobutyric acid content increased while the stearic acid (C18:0) content was decreased in the AA group. Citrobacter has been identified as a microorganism that can cause intestinal

inflammation; thus, *Citrobacter rodentium* is inextricably linked to human immune cells, especially dendritic cells and CD4+ T cells[26]. *Citrobacter koseri*, a subspecies of Citrobacter, stimulates dendritic cells to induce IL-33 through massive ATP production[27]. Plasmacytoid dendritic cells (pDCs) are the main dendritic cells upregulated upon stimulation in *Citrobacter rodentium* infection[28]. Upregulation of the mDC/pDC ratio in aplastic anaemia patients has also been validated, whereby the dendritic cell response due to the downregulation of Citrobacter abundance and immune cell changes in the AA group in the barrier coincide[29]. The involvement of short-chain fatty acids can enhance the induction of Th1 and Th17 cells during *Citrobacter rodentium* infection in mice[30]. In our study, the isobutyric acid content was upregulated in the AA group and negatively correlated with Citrobacter abundance, coinciding with the upregulation of Th17 cells in AA patients. Downregulation of murine Treg cells enhances *Citrobacter rodentium* susceptibility, whereas infection with *Citrobacter rodentium* in the intestinal cells of mice lacking Treg cells elicits a strong Th17 response [31]. Moreover, the branched palmitic acid esters of hydroxy stearic acids (PAHSAs), which induce colonic T cell activation and inhibit proinflammatory cytokine and chemokine expression in mice, attenuate dendritic cell activation and subsequent T cell proliferation and Th1 polarization in vitro[32]. In our study, the stearic acid content and Citrobacter level were downregulated at the same time, and both were positively correlated, in accordance with the conclusion of the above study. Taken together, these results suggest that the unusual presentation of stearic and isobutyric acids in patients with aplastic anaemia is most likely related to its immunopathogenic mechanisms. Although little research has pointed out the correlation between isobutyric acid and human immunity, studies on short-chain fatty acids (SCFAs) derived from microbes are not rare. Studies have shown that SCFAs promote cell metabolism and enhance the memory potential of activated CD8+ T cells [33]. Patients with aplastic anaemia show downregulation of Treg cells and upregulation of Th17 cells [21,34]. Previous studies have suggested that aplastic anaemia patients are susceptible to Citrobacter, but in our study, Citrobacter abundance was downregulated; however, the immune changes induced by Citrobacter infection were consistent, which suggested that Citrobacter infection might be the driving factor of aplastic anaemia. Citrobacter infection may also be involved in energy metabolism in patients with aplastic anaemia and thus in the gut microenvironment of aplastic anaemia. Citrobacter controls the production of H2O2 by the NADPH oxidase NOX1 to provide growth conditions for other aerobic bacteria early after infection [35]. The intestinal epithelium absorption of acylcarnitine is impaired by Citrobacter, and then the aerobic metabolism of intestinal epithelial cells is affected [36]. Lysine degradation, which has the same fatty acid correlation with Citrobacter, is a process of energy metabolism that refers to the conversion of lysine to acetyl-coA. Another closely related biosynthesis pathway of betaine is an independent biosynthesis process that focuses on plants. Betaine is the end product of choline oxidation in the human body. Methionine is involved in the biosynthesis of the gut microenvironment, and its role in the formation of the gut microenvironment is unknown. In conclusion, it is reasonable to hypothesize that Citrobacter and its related fatty acids mainly influence the immunopathogenesis of aplastic anaemia and greatly influence the formation of the intestinal microenvironment; therefore, Citrobacter is very likely to be a pathogenic factor of aplastic anaemia and has great potential and research value in aplastic anaemia.

We also noted a decrease in the abundance of Nematoda in eukaryotes identified in aplastic anaemia patients and a decrease in the abundances of Enoplea, Trichinellida, Trichuridae, Enterocytozoon and Trichuris within this phylum, which were negatively correlated with the contents of eicosenoate, docosatetraenoate and 10-transsheptadecenoate in the plasma. In addition, the number of Mycoavidus species [37] in the nematode-related bacterial community was decreased and negatively correlated with docosadienoate and docosatetraenoate. Previous studies have shown that nematodes are primarily associated with unsaturated fatty acids, consistent with our findings. The nematode Caenorhabditis elegans stores unsaturated fatty acids in droplets in its subcutaneous and intestinal cells [38]. Additionally, 18-carbon PUFAs affect basal innate immune function, the p38 MAP kinase pathway and the transcription of fat-3-regulated genes through the nematode Caenorhabditis elegans to modulate intestinal infection and the expression of genes involved in the stress response, thereby affecting the organism's ability to defend against bacterial infection [39]. Helminth-induced chronic infection can increase anti-inflammatory cytokine secretion and suppress Treg cell activity and increase short-chain fatty acid (SCFA) production [40]. The loss of C. elegans fat-1 expression inhibits lipid droplet formation and selectively disrupts peroxisomes and apical endosomes. Lipid analysis in fat-1-deficient nematodes revealed a significant reduction in heptadecaenoic acid, while other major FAs were unaffected [41]. Caenorhabditis elegans intestinal colonization causes protein homeostasis disruption, which can be improved by butyrate [42]. Two peptides, ACAN1 and NAK1, derived from the nematode phylum, have immunomodulatory functions and can inhibit the proliferation of CD4+ T cells and the production of IL-2 and TNF [43]. Therefore, we can conclude that the nematode phylum acts as a mediator in the human body. On the one hand, the nematode phylum can directly participate in the synthesis and storage of fatty acids; on the other hand, it serves as the link between fatty acid metabolism and immune regulation. The abundance of nematode phylum microbes in the faeces of patients with aplastic anaemia was decreased, as were the levels of several fatty acids that showed negative correlations with it, although there was a negative correlation between the two. There should be a complex interaction mechanism among them. First, the decline in nematode microbiome levels may be due to an increased proportion of T cells in the peripheral blood of immunocompromised patients with aplastic anaemia. Inhibition of the nematode phyla decreased the colonization of long-chain fatty acids in the intestinal epithelium and increased the contents of long-chain fatty acids in the peripheral blood, such that there was a negative correlation between them. We hypothesize that the decrease in fatty acid contents in the peripheral blood may be due to other microorganisms or microbial associations. Docosadienoate was negatively correlated with N-glycan biosynthesis, and N-glycan biosynthesis was negatively correlated with nematode-related microorganisms. N-glycan biosynthesis is associated with weight loss [44]; in other words, there may be a negative correlation with the biosynthesis of fatty acids, which can confirm the negative change in the fatty acids described above and nematode microbial abundance.

The decrease in microbial abundance of the Catenibacterium genus, including *Catenibacterium mitsuokaiin* species, in the bacterial kingdom was also noTab. In the AA group, there was a positive correlation between the docosatetraenoate content in both the plasma and supernatant, and the docosatetraenoate content was also positively correlated with downregulated ubiquinone and other terpenoid-quinone biosynthesis pathways. Previous studies have shown that the microbial abundance of this genus is similarly downregulated in inflammatory bowel disease patients[45] and in aplastic anaemia patients in our study, suggesting that it may have some relevance for immunity. In a study of fructose fermentation by faecal microorganisms in vitro, the abundance of Catenibacterium increased with increasing SCFA contents, especially with the increase in butyric acid [46,47]. A study of the gut flora in obese patients found an elevated microbial abundance of Catenibacterium and high plasma levels of short-chain fatty acids, corroborating the above

findings [48]. As mentioned earlier, the impact of short-chain fatty acid synthesis on the immune response is gradually being recognized. Valeric acid and butyric acid enhance the antitumour activity of cytotoxic T lymphocytes (CTLs) and chimeric antigen receptor (car) T cells through metabolic and epigenetic reprogramming [49]. SCFAs promote apoptosis by promoting aryl hydrocarbon receptor (AhR) and hypoxia-inducible factor 1α (HIF1α) expression to upregulate IL-22 production by CD4+ T cells [50]. Microbiota-derived metabolites can modulate the suppressive function of Bregs [51]. Butyrate produced by the intestinal flora regulates antigen presentation and radiotherapy following DC-induced antitumour immune responses[52]. As previously mentioned, these immune cells have been implicated in the pathogenesis of aplastic anaemia[53]. Furthermore, docosatetraenoate is positively correlated with ubiquinone and other terpenoid quinone biosynthesis pathways, and recent studies have shown that ubiquinone and other terpenoid quinone biosynthesis pathways are often linked to the synthesis of unsaturated fatty acids[54]. We speculate that the immune abnormalities caused by the decline in the abundance of Catenibacterium mitsuokai species at the Catenibacterium genus may be involved in the pathogenesis of aplastic anaemia; furthermore, the biotransformation of docosatetraenoate is influenced by ubiquinone and other terpenoid quinone biosynthesis pathways. Docosatetraenoate, a long-chain unsaturated fatty acid that cannot be synthesized in the body, has various functions and is involved in the regulation of inflammation and bone destruction through the cyclooxygenase and lipoxygenase pathways [55]. Long-chain unsaturated fatty acids are also involved in the regulation of bone marrow-derived macrophage activity by regulating long-chain acyl-coenzyme A synthetases (ACSLs) [56] and have a protective effect on drug-induced bone destruction [57,58]. In conclusion, unsaturated fatty acids may be involved in the regulation of the inflammatory response and may affect the bone marrow microenvironment. Therefore, the downregulation of docosatetraenoate may be involved in both immune response enhancement and the process of bone destruction and marrow steatosis in aplastic anaemia patients. Although no specific studies have been performed, we believe that unsaturated fatty acids have immense potential in the study of the pathogenesis of aplastic anaemia.

The abundance of Enhydrobacter species was increased in the AA group and was positively correlated with docosadienoatein in the plasma and docosatetraenoate in bone marrow supernatants. Moreover, the abundance of Enhydrobacter aerosaccus species in the Enhydrobacter genus had a positive correlation with phenylalanine, tyrosine and tryptophan biosynthesis but a negative correlation with N-glycan biosynthesis. Previous studies have shown that the Enhydrobacter genus is also abundant in gastrointestinal metaplasia and associated with carcinoma of the head of pancreas (CHP) [59,60]. In in vitro synthesis experiments, an aminotransferase derived from the bacterium Enhydrobacter catalysed the synthesis of L-phenylalanine by using 3-GABA as an amino donor[61], as confirmed by our results in patients with aplastic anaemia. Studies have shown that L-phenylalanine metabolism is associated with fatty acid synthesis[62]. Il-10 has been shown to directly inhibit the function of CD8+ T cells by increasing the number of n-glycan branches to decrease antigenic sensitivity [63]. Additionally, CD8+ cell function was upregulated in patients with aplastic anaemia, and our study showed that the abundance of species in the n-branching glycan biosynthesis pathway was decreased in the AA group, consistent with previous findings. N-glycan biosynthesis is also involved in the migration of bone marrow-derived mesenchymal stem cells[64]. Downregulation of N-glycan biosynthesis may inhibit the migration of MSCs outside the bone marrow in aplastic anaemia patients, thus prompting the MSC source to differentiate into adipocytes directly inside the bone marrow and complete the marrow lipidation process. Although there is no research to prove this hypothesis, we still believe there is great research potential. As previously mentioned, long-chain unsaturated fatty acids may be involved in regulating the immune response and preventing bone destruction. However, here, we believe that long-chain unsaturated fatty acids primarily affect the process of steatosis in the bone marrow through their role in the bone marrow microenvironment in aplastic anaemia patients. Enhydrobacter (also associated with the presence of long-chain fatty acids) was positively and negatively associated with two biosynthetic pathways, both of which were positively associated with docosadienoate in the plasma and docosatetraenoate in the bone marrow, respectively. Therefore, it is reasonable to hypothesize that this microbe is more likely to affect the aplastic anaemia process than the immune response.

Conclusion

Our study is the first time that apply Metagenomic to the study of aplastic anemia.Based on the CG-MS lipid detection technique, we found that there were differences in lipid metabolism between the AA group and the NC group, whether short chain fatty acids or medium and long chain fatty acids;Differences in fatty acid metabolism are reflected both in bone marrow supernatants and peripheral plasma, with more significant differences in long-chain fatty acids in peripheral plasma than in short chain fatty acids in bone marrow supernatants;Most fatty acids, whether medium and long chain fatty acids or short chain fatty acids showed a decreasing trend in the disease group, demonstrating that the metabolism of the disease group as a whole was attenuated;

Microbial metabolic alterations are associated with alterations in fatty acids, not only in short but also in long-chain fatty acids, demonstrating that microbial metabolism similarly affects long-chain fatty acid synthesis and metabolism;The interrelationship between Citrobacter spp stearic acid (c18:0), isobutyric acid, and lysine degradation and betaine biosynthesis pathway suggests that Citrobacter positively regulated stearic acid biosynthesis and precisely negatively regulated isobutyric acid production by these two pathways.The interrelationship between catenibacterium_mitsuokai species at Catenibacterium, cis-7,10,13,16-docosatetraenoic acid (c22:4), ubiquinone and other terpenoid quinones pathway suggests that Catenibacterium negatively regulate cis-7,10,13,16-docosatetraenoic acid by biosynthesis of ubiquinone and other terpenoid quinones.The intercorrelation between the abundance of Enhydrobacter genus and Enhydrobacter_aerosaccus species, cis-13,16-docosadienoic acid in peripheral plasma, cis-7,10,13,16-docosatetraenoic acid in bone marrow supernatant, tyrosine and tryptophan biosynthesis pathway suggests that the genus aquabacterium is associated with two long-chain fatty acids through tyrosine and tryptophan biosynthetic pathway modulation in the disease group.From the point of view of immunity, citreobacilli plays an important role in the pathogenesis of aplastic anemia. We speculate that it may act as a driving factor for aplastic anemia.From the perspective of lipid metabolism, docosanpoly unsaturated fatty acids are of significant relevance to the microbiota in the patient group, and we speculate that docosanpoly unsaturated fatty acids may serve as mediators of microbiota regulated medium - and long-chain fatty acid metabolism.

Overall, our study not only sheds light on the possibility that Citrobacter infection may function as an aplastic anaemia agent but also revealed the potential role of stearate in the immunopathogenesis of aplastic anaemia. In addition, our study demonstrates the potential roles of 22 unsaturated fatty acids in aplastic anaemia. Unsaturated fats are not only involved in the metabolism of fibroblasts in the bone marrow, thus affecting the formation of the bone

marrow microenvironment and participation in the process of bone marrow steatosis, but may also be involved in the regulation of immune cells in the peripheral blood to participate in disease progression in aplastic anaemia patients. Our study provides insights into the pathogenesis of aplastic anaemia and, more importantly, sheds light on the aetiology of aplastic anaemia.

Abbreviations

AA	Aplastic anemia
NC	Normal control
PCR	Polymerase chain reaction
PCA	Principal Component Analysis
PCR	Polymerase chain reaction
PLS-DA	Partial Least Squares-Discriminant Analysis
OPLS-DA	Orthogonal Projections to Latent Structures Discriminant Analysis
GC-MS	gas chromatography-mass spectrometry
C6:0	Caproate
C8:0	Caprylate
C10:0	Caprate
C11:0	Unndecanoate
C12:0	Laurate
C13:0	Tridecanoate
C14:0	Myristate
C14:1T	Myristelaidate
C14:1	Myristoleate
C15:0	Pentadecanoate
C15:1T	10-Transpentadecenoate
C15:1	10-Pentadecenoate
C16:0	Palmitate
C16:1T	Palmitelaidate
C16:1	Palmitoleate
C17:0	Heptadecanoate
C17:1T	10-Transsheptadecenoate
C17:1	10-Heptadecenoate
C18:0	Stearate
C18:1N12T	Petroselaidate
C18:1N9T	Elaidate
C18:1N7T	Transvaccenate
C18:1N12	Petroselinate
C18:1N9C	Oleate
C18:1N7	Vaccenate
C18:2N6T	Linoelaidate
C19:1N12T	7-Transnonadecenoate
C19:1N9T	10-Transnonadecenoate
C18:2N6	Linoleate
C20:0	Arachidate
C18:3N6	Gamma Linolenate
C20:1T	Trans 11-Eicosenoate
C20:1	11-Eicosenoate
C18:3N3	Alpha Linolenate
C21:0	Heneicosanoate

C20:2	11-14 Eicosadienoate
C22:0	Behenate
C20:3N6	Homogamma Linolenate
C22:1N9T	Brassidate
C22:1N9	Erucate
C20:3N3	11-14-17 Eicosatrienoate
C20:4N6	Arachidonate
C23:0	Tricosanoate
C22:2	Docosadienoate
C20:5N3	Eicosapentaenoate
C24:0	Lignocerate
C24:1	Nervonoate
C22:4	Docosatetraenoate
C22:5N6	Docosapentaenoate
C22:5N3	Docosapentaenoate
C22:6N3	Docosahexaenoate

Declarations

Ethics approval and consent to participate

This study is approved by the Tianjin Medical University General Hospital Ethical Committee. Ethical NO. IRB2022-WZ-003

Consent for publication

Not applicable

Availability of data and materials

All data generated or analysed during this study are included in this published article [and its supplementary information files].

Competing interests

All authors declare no competing interests.

Funding

This work was supported by National Natural Science Foundation of China(Grant Nos. 81870101,81870117 and 81800120).

Authors' contributions

Xiaoyu Zhao and Chaomeng Wang analyzed and interpreted data;Xiaoyu Zhao, Chenchen Liu and Nan Jian performed statistical analysis and wrote the manuscript; Tian Zhang, Shaoxue Ding, Tong Chen collected datas;Xiaoyu Zhao, Yingying Sun, Bingnan Liu, Dan Lu, Yingying Chen and Liping Yang performed research and completed the experimental procedures; Chunyan Liu and Rong Fu are corresponding authors and designed our research.

Acknowledgements

Thanks for National Natural Science Foundation of China for its financial support, the technical support provided by sequencing company and Experimental site provided by Department of Hematology Laboratory of Tianjin Medical University General Hospital.

References

1. Young NS. Aplastic Anemia. *N Engl J Med*. Oct 25 2018;379(17):1643-1656. doi:10.1056/NEJMra1413485
2. Stechschulte LA, Ge C, Hinds TD, Jr., Sanchez ER, Franceschi RT, Lecka-Czernik B. Protein Phosphatase PP5 Controls Bone Mass and the Negative Effects of Rosiglitazone on Bone through Reciprocal Regulation of PPARgamma (Peroxisome Proliferator-activated Receptor gamma) and RUNX2 (Runt-related Transcription Factor 2). *J Biol Chem*. Nov 18 2016;291(47):24475-24486. doi:10.1074/jbc.M116.752493

3. Wang FS, Ko JY, Yeh DW, Ke HC, Wu HL. Modulation of Dickkopf-1 attenuates glucocorticoid induction of osteoblast apoptosis, adipocytic differentiation, and bone mass loss. *Endocrinology*. Apr 2008;149(4):1793-801. doi:10.1210/en.2007-0910
4. F.-Z. Chang QW, Q. Zhang, L.-L. Chang, W. Li. Omega-3 polyunsaturated fatty acid inhibits the malignant progression of hepatocarcinoma by inhibiting the Wnt/β-catenin pathway. review. *European Review for Medical and Pharmacological Sciences*. 2018;2018; 22 (14): 4500-4508:4500-4508. doi:10.26355/eurrev_201807_15504
5. Rharass T, Lucas S. MECHANISMS IN ENDOCRINOLOGY: Bone marrow adiposity and bone, a bad romance? *Eur J Endocrinol*. Oct 1 2018;179(4):R165-R182. doi:10.1530/EJE-18-0182
6. Al Saedi A, Bermeo S, Plotkin L, Myers DE, Duque G. Mechanisms of palmitate-induced lipotoxicity in osteocytes. *Bone*. Oct 2019;127:353-359. doi:10.1016/j.bone.2019.06.016
7. Shao Y, Qi W, Zhang X, et al. Plasma Metabolomic and Intestinal Microbial Analyses of Patients With Severe Aplastic Anemia. *Front Cell Dev Biol*. 2021;9:669887. doi:10.3389/fcell.2021.669887
8. Derrien M, Vaughan EE, Plugge CM, de Vos WM. Akkermansia muciniphila gen. nov., sp. nov., a human intestinal mucin-degrading bacterium. *Int J Syst Evol Microbiol*. Sep 2004;54(Pt 5):1469-1476. doi:10.1099/ijs.0.02873-0
9. Frost G, Sleeth ML, Sahuri-Arisoylu M, et al. The short-chain fatty acid acetate reduces appetite via a central homeostatic mechanism. *Nat Commun*. Apr 29 2014;5:3611. doi:10.1038/ncomms4611
10. de Smit SM, de Leeuw KD, Buisman CJN, Strik D. Continuous n-valerate formation from propionate and methanol in an anaerobic chain elongation open-culture bioreactor. *Biotechnol Biofuels*. 2019;12:132. doi:10.1186/s13068-019-1468-x
11. Donohoe DR, Collins LB, Wali A, Bigler R, Sun W, Bultman SJ. The Warburg effect dictates the mechanism of butyrate-mediated histone acetylation and cell proliferation. *Mol Cell*. Nov 30 2012;48(4):612-26. doi:10.1016/j.molcel.2012.08.033
12. van der Hee B, Wells JM. Microbial Regulation of Host Physiology by Short-chain Fatty Acids. *Trends Microbiol*. Aug 2021;29(8):700-712. doi:10.1016/j.tim.2021.02.001
13. Marsh JC, Ball SE, Cavenagh J, et al. Guidelines for the diagnosis and management of aplastic anaemia. *Br J Haematol*. Oct 2009;147(1):43-70. doi:10.1111/j.1365-2141.2009.07842.x
14. Young NS, Calado RT, Scheinberg P. Current concepts in the pathophysiology and treatment of aplastic anemia. *Blood*. Oct 15 2006;108(8):2509-19. doi:10.1182/blood-2006-03-010777
15. Kordasti S, Costantini B, Seidl T, et al. Deep phenotyping of Tregs identifies an immune signature for idiopathic aplastic anemia and predicts response to treatment. *Blood*. Sep 1 2016;128(9):1193-205. doi:10.1182/blood-2016-03-703702
16. Kordasti S, Marsh J, Al-Khan S, et al. Functional characterization of CD4+ T cells in aplastic anemia. *Blood*. Mar 1 2012;119(9):2033-43. doi:10.1182/blood-2011-08-368308
17. Grover P, Goel PN, Greene MI. Regulatory T Cells: Regulation of Identity and Function. *Front Immunol*. 2021;12:750542. doi:10.3389/fimmu.2021.750542
18. Sun Y, Wu C, Liu C, et al. Myeloid dendritic cells in severe aplastic anemia patients exhibit stronger phagocytosis. *J Clin Lab Anal*. Oct 18 2021:e24063. doi:10.1002/jcla.24063
19. Liu B, Shao Y, Liang X, et al. CTLA-4 and HLA-DQ are key molecules in the regulation of mDC-mediated cellular immunity by Tregs in severe aplastic anemia. *J Clin Lab Anal*. Oct 2020;34(10):e23443. doi:10.1002/jcla.23443
20. Liu C, Zheng M, Wang T, et al. PKM2 Is Required to Activate Myeloid Dendritic Cells from Patients with Severe Aplastic Anemia. *Oxid Med Cell Longev*. 2018;2018:1364165. doi:10.1155/2018/1364165
21. de Latour RP, Visconte V, Takaku T, et al. Th17 immune responses contribute to the pathophysiology of aplastic anemia. *Blood*. Nov 18 2010;116(20):4175-84. doi:10.1182/blood-2010-01-266098
22. Wu L, Mo W, Zhang Y, et al. Impairment of hematopoietic stem cell niches in patients with aplastic anemia. *Int J Hematol*. Dec 2015;102(6):645-53. doi:10.1007/s12185-015-1881-2
23. Gao F, Chiu SM, Motan DA, et al. Mesenchymal stem cells and immunomodulation: current status and future prospects. *Cell Death Dis*. Jan 21 2016;7:e2062. doi:10.1038/cddis.2015.327
24. Chao YH, Peng CT, Harn HJ, Chan CK, Wu KH. Poor potential of proliferation and differentiation in bone marrow mesenchymal stem cells derived from children with severe aplastic anemia. *Ann Hematol*. Jul 2010;89(7):715-23. doi:10.1007/s00277-009-0892-6
25. Chao YH, Tsai C, Peng CT, et al. Cotransplantation of umbilical cord MSCs to enhance engraftment of hematopoietic stem cells in patients with severe aplastic anemia. *Bone Marrow Transplant*. Oct 2011;46(10):1391-2. doi:10.1038/bmt.2010.305
26. Yang W, Liu H, Xu L, et al. GPR120 Inhibits Colitis Through Regulation of CD4(+) T Cell Interleukin 10 Production. *Gastroenterology*. Sep 16 2021;doi:10.1053/j.gastro.2021.09.018
27. Kataoka H, Mori T, Into T. Citrobacter koseri stimulates dendritic cells to induce IL-33 expression via abundant ATP production. *J Med Microbiol*. Mar 2021;70(3)doi:10.1099/jmm.0.001303
28. Poysti S, Silojarvi S, Toivonen R, Hanninen A. Plasmacytoid dendritic cells regulate host immune response to Citrobacter rodentium induced colitis in colon-draining lymph nodes. *Eur J Immunol*. Mar 2021;51(3):620-625. doi:10.1002/eji.202048714
29. Zonghong S, Meifeng T, Huaquan W, et al. Circulating myeloid dendritic cells are increased in individuals with severe aplastic anemia. *Int J Hematol*. Feb 2011;93(2):156-162. doi:10.1007/s12185-010-0761-z

30. Park J, Kim M, Kang SG, et al. Short-chain fatty acids induce both effector and regulatory T cells by suppression of histone deacetylases and regulation of the mTOR-S6K pathway. *Mucosal Immunol*. Jan 2015;8(1):80-93. doi:10.1038/mi.2014.44
31. Wang Z, Friedrich C, Hagemann SC, et al. Regulatory T cells promote a protective Th17-associated immune response to intestinal bacterial infection with C. rodentium. *Mucosal Immunol*. Nov 2014;7(6):1290-301. doi:10.1038/mi.2014.17
32. Lee J, Moraes-Vieira PM, Castoldi A, et al. Branched Fatty Acid Esters of Hydroxy Fatty Acids (FAHFAs) Protect against Colitis by Regulating Gut Innate and Adaptive Immune Responses. *J Biol Chem*. Oct 14 2016;291(42):22207-22217. doi:10.1074/jbc.M115.703835
33. Bachem A, Makhlouf C, Binger KJ, et al. Microbiota-Derived Short-Chain Fatty Acids Promote the Memory Potential of Antigen-Activated CD8(+) T Cells. *Immunity*. Aug 20 2019;51(2):285-297 e5. doi:10.1016/j.immuni.2019.06.002
34. Shi J, Ge M, Lu S, et al. Intrinsic impairment of CD4(+)CD25(+) regulatory T cells in acquired aplastic anemia. *Blood*. Aug 23 2012;120(8):1624-32. doi:10.1182/blood-2011-11-390708
35. Miller BM, Liou MJ, Zhang LF, et al. Anaerobic Respiration of NOX1-Derived Hydrogen Peroxide Licenses Bacterial Growth at the Colonic Surface. *Cell Host Microbe*. Dec 9 2020;28(6):789-797 e5. doi:10.1016/j.chom.2020.10.009
36. Smith SA, Ogawa SA, Chau L, et al. Mitochondrial dysfunction in inflammatory bowel disease alters intestinal epithelial metabolism of hepatic acylcarnitines. *J Clin Invest*. Jan 4 2021;131(1)doi:10.1172/JCI133371
37. Palomares-Rius JE, Gutierrez-Gutierrez C, Mota M, et al. 'Candidatus Xiphinematincola pachtaicus' gen. nov., sp. nov., an endosymbiotic bacterium associated with nematode species of the genus Xiphinema (Nematoda, Longidoridae). *Int J Syst Evol Microbiol*. Jul 2021;71(7)doi:10.1099/ijsem.0.004888
38. Bouyanfif A, Jayarathne S, Koboziev I, Moustaid-Moussa N. The Nematode Caenorhabditis elegans as a Model Organism to Study Metabolic Effects of omega-3 Polyunsaturated Fatty Acids in Obesity. *Adv Nutr*. Jan 1 2019;10(1):165-178. doi:10.1093/advances/nmy059
39. Ge H, Li X, Weiszmann J, et al. Activation of G protein-coupled receptor 43 in adipocytes leads to inhibition of lipolysis and suppression of plasma free fatty acids. *Endocrinology*. Sep 2008;149(9):4519-26. doi:10.1210/en.2008-0059
40. Zaiss MM, Rapin A, Lebon L, et al. The Intestinal Microbiota Contributes to the Ability of Helminths to Modulate Allergic Inflammation. *Immunity*. Nov 17 2015;43(5):998-1010. doi:10.1016/j.immuni.2015.09.012
41. Li Y, Wang C, Huang Y, et al. C. Elegans Fatty Acid Two-Hydroxylase Regulates Intestinal Homeostasis by Affecting Heptadecenoic Acid Production. *Cell Physiol Biochem*. 2018;49(3):947-960. doi:10.1159/000493226
42. Walker AC, Bhargava R, Vaziriyan-Sani AS, et al. Colonization of the Caenorhabditis elegans gut with human enteric bacterial pathogens leads to proteostasis disruption that is rescued by butyrate. *PLoS Pathog*. May 2021;17(5):e1009510. doi:10.1371/journal.ppat.1009510
43. Smallwood TB, Navarro S, Cristofori-Armstrong B, et al. Synthetic hookworm-derived peptides are potent modulators of primary human immune cell function that protect against experimental colitis in vivo. *J Biol Chem*. Jul 2021;297(1):100834. doi:10.1016/j.jbc.2021.100834
44. Greto VL, Cvetko A, Stambuk T, et al. Extensive weight loss reduces glycan age by altering IgG N-glycosylation. *Int J Obes (Lond)*. Jul 2021;45(7):1521-1531. doi:10.1038/s41366-021-00816-3
45. Masoodi I, Alshanqeeti AS, Ahmad S, et al. Microbial dysbiosis in inflammatory bowel diseases: results of a metagenomic study in Saudi Arabia. *Minerva Gastroenterol Dietol*. Sep 2019;65(3):177-186. doi:10.23736/S1121-421X.19.02576-5
46. Liu C, Du P, Cheng Y, et al. Study on fecal fermentation characteristics of aloe polysaccharides in vitro and their predictive modeling. *Carbohydr Polym*. Mar 15 2021;256:117571. doi:10.1016/j.carbpol.2020.117571
47. Sayago-Ayerdi SG, Zamora-Gasga VM, Venema K. Changes in gut microbiota in predigested Hibiscus sabdariffa L calyces and Agave (Agave tequilana weber) fructans assessed in a dynamic in vitro model (TIM-2) of the human colon. *Food Res Int*. Jun 2020;132:109036. doi:10.1016/j.foodres.2020.109036
48. Martinez-Cuesta MC, Del Campo R, Garriga-Garcia M, Pelaez C, Requena T. Taxonomic Characterization and Short-Chain Fatty Acids Production of the Obese Microbiota. *Front Cell Infect Microbiol*. 2021;11:598093. doi:10.3389/fcimb.2021.598093
49. Luu M, Riester Z, Baldrich A, et al. Microbial short-chain fatty acids modulate CD8(+) T cell responses and improve adoptive immunotherapy for cancer. *Nat Commun*. Jul 1 2021;12(1):4077. doi:10.1038/s41467-021-24331-1
50. Yang W, Yu T, Huang X, et al. Intestinal microbiota-derived short-chain fatty acids regulation of immune cell IL-22 production and gut immunity. *Nat Commun*. Sep 8 2020;11(1):4457. doi:10.1038/s41467-020-18262-6
51. Rosser EC, Piper CJM, Matei DE, et al. Microbiota-Derived Metabolites Suppress Arthritis by Amplifying Aryl-Hydrocarbon Receptor Activation in Regulatory B Cells. *Cell Metab*. Apr 7 2020;31(4):837-851 e10. doi:10.1016/j.cmet.2020.03.003
52. Uribe-Herranz M, Rafail S, Beghi S, et al. Gut microbiota modulate dendritic cell antigen presentation and radiotherapy-induced antitumor immune response. *J Clin Invest*. Jan 2 2020;130(1):466-479. doi:10.1172/JCI124332
53. Javan MR, Saki N, Moghimian-Boroujeni B. Aplastic anemia, cellular and molecular aspects. *Cell Biol Int*. Aug 18 2021;doi:10.1002/cbin.11689
54. Chen J, Tang H, Li T, et al. Comprehensive Analysis of the Expression, Prognosis, and Biological Significance of OVOLs in Breast Cancer. *Int J Gen Med*. 2021;14:3951-3960. doi:10.2147/IJGM.S326402
55. Pino AM, Rodriguez JP. Is fatty acid composition of human bone marrow significant to bone health? *Bone*. Jan 2019;118:53-61. doi:10.1016/j.bone.2017.12.014
56. Kuwata H, Nakatani E, Shimbara-Matsubayashi S, et al. Long-chain acyl-CoA synthetase 4 participates in the formation of highly unsaturated fatty acid-containing phospholipids in murine macrophages. *Biochim Biophys Acta Mol Cell Biol Lipids*. Nov 2019;1864(11):1606-1618.

doi:10.1016/j.bbalip.2019.07.013

57. Gao B, Han YH, Wang L, et al. Eicosapentaenoic acid attenuates dexamethasome-induced apoptosis by inducing adaptive autophagy via GPR120 in murine bone marrow-derived mesenchymal stem cells. *Cell Death Dis*. May 26 2016;7:e2235. doi:10.1038/cddis.2016.144
58. Fan CM, Su YW, Howe PR, Xian CJ. Long Chain Omega-3 Polyunsaturated Fatty Acid Supplementation Protects Against Adriamycin and Cyclophosphamide Chemotherapy-Induced Bone Marrow Damage in Female Rats. *Int J Mol Sci*. Feb 6 2018;19(2)doi:10.3390/ijms19020484
59. Mei QX, Huang CL, Luo SZ, Zhang XM, Zeng Y, Lu YY. Characterization of the duodenal bacterial microbiota in patients with pancreatic head cancer vs. healthy controls. *Pancreatology*. Jun 2018;18(4):438-445. doi:10.1016/j.pan.2018.03.005
60. Gong J, Li L, Zuo X, Li Y. Change of the duodenal mucosa-associated microbiota is related to intestinal metaplasia. *BMC Microbiol*. Dec 9 2019;19(1):275. doi:10.1186/s12866-019-1666-5
61. Feng X, Guo J, Zhang R, et al. An Aminotransferase from Enhydrobacter aerosaccus to Obtain Optically Pure beta-Phenylalanine. *ACS Omega*. Apr 14 2020;5(14):7745-7750. doi:10.1021/acsomega.9b03416
62. Lyu X, Yan K, Chen W, et al. The characterization of metabolites alterations in white adipose tissue of diabetic GK Rats after ileal transposition surgery by an untargeted metabolomics approach. *Adipocyte*. Dec 2021;10(1):275-284. doi:10.1080/21623945.2021.1926139
63. Smith LK, Boukhaled GM, Condotta SA, et al. Interleukin-10 Directly Inhibits CD8(+) T Cell Function by Enhancing N-Glycan Branching to Decrease Antigen Sensitivity. *Immunity*. Feb 20 2018;48(2):299-312 e5. doi:10.1016/j.immuni.2018.01.006
64. Alonso-Garcia V, Chaboya C, Li Q, et al. High Mannose N-Glycans Promote Migration of Bone-Marrow-Derived Mesenchymal Stromal Cells. *Int J Mol Sci*. Sep 29 2020;21(19)doi:10.3390/ijms21197194

Figures

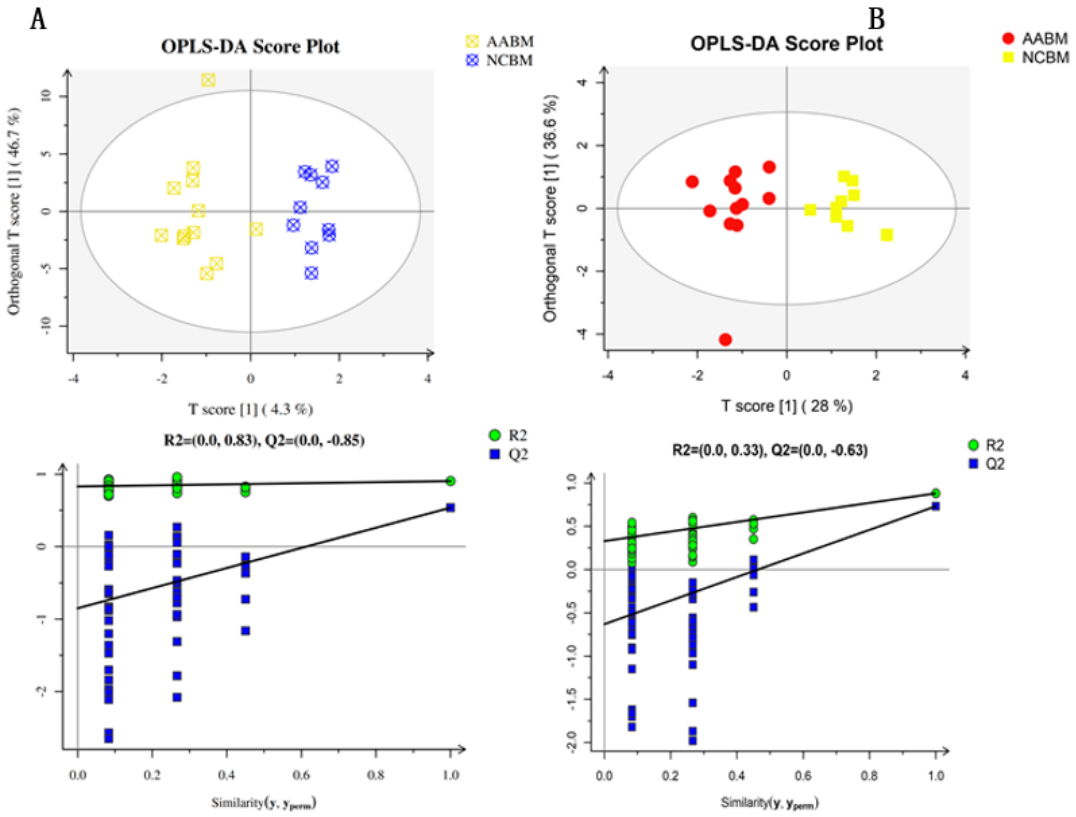

Figure 1

A. OPLS-DA analysis of medium and long-chain fatty acids in the bone marrow;B. OPLS-DA analysis of short-chain fatty acids in the bone marrow

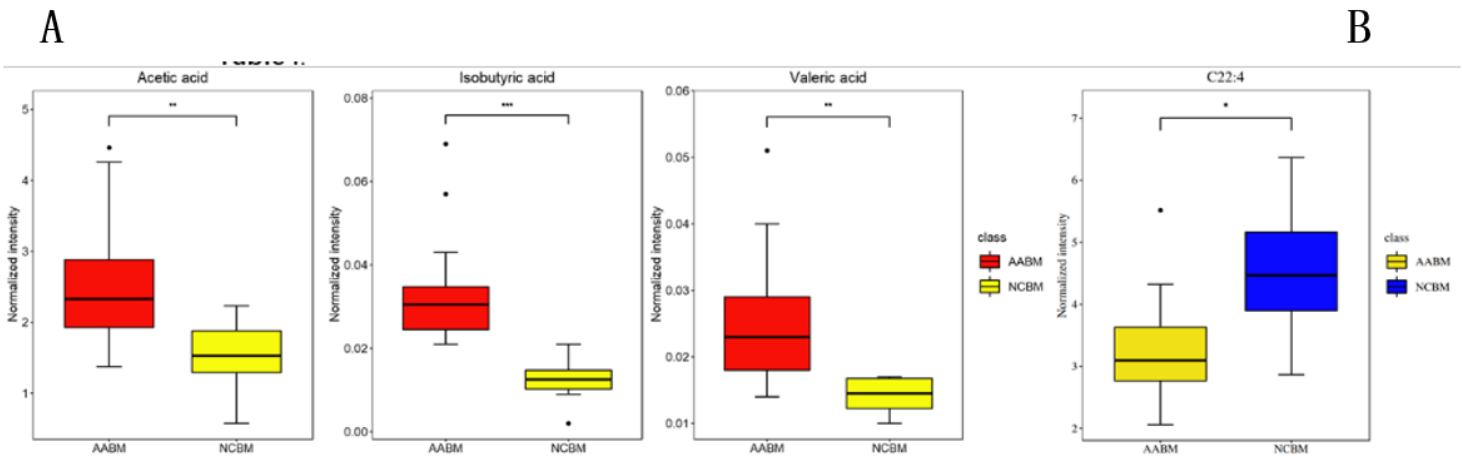

Figure 2

A.3 changed short-chain fatty acids in AA group in the bone marrow .B. docosatetraenoate (C22:4) decreased in AA group in the bone marrow.

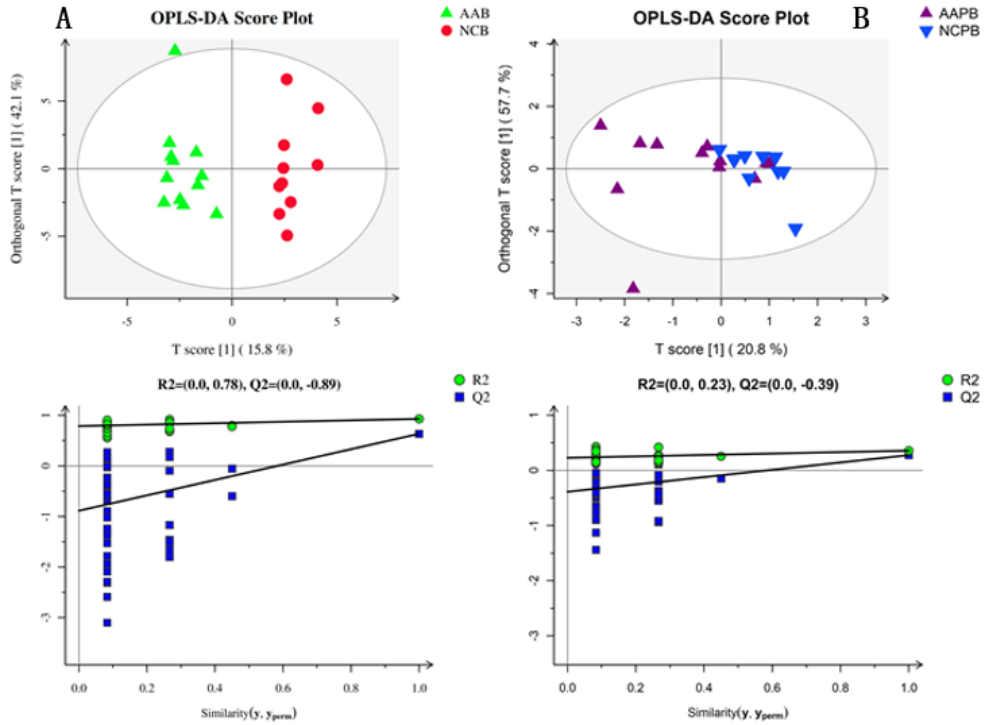

Figure 3

A. OPLS-DA analysis of medium and long-chain fatty acids in plasma;B. OPLS-DA analysis of short-chain fatty acids in plasma

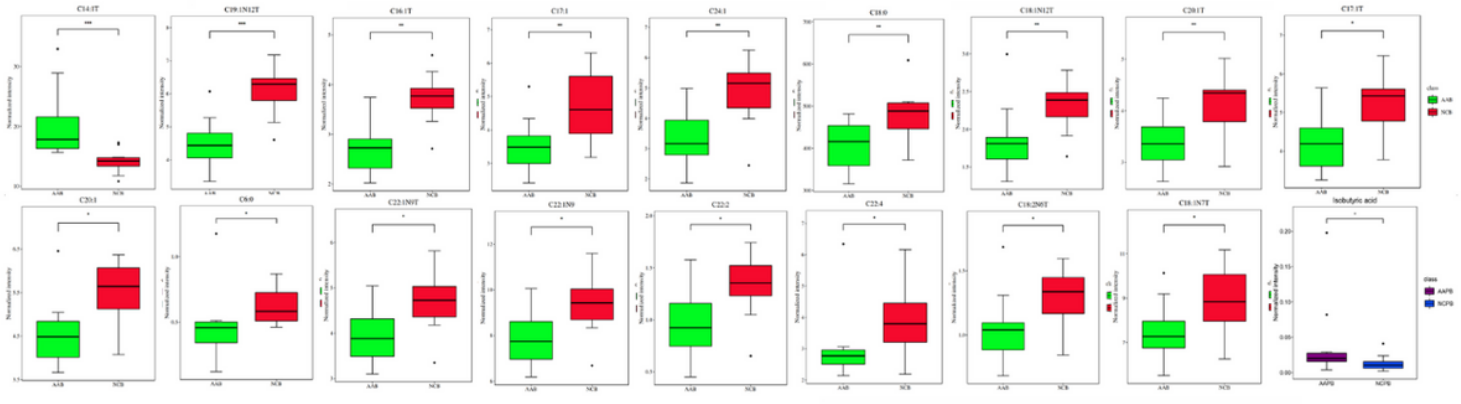

Figure 4

changed fatty acids(including long-chain fatty acids and short-chain fatty acids) in AA group in plasm.

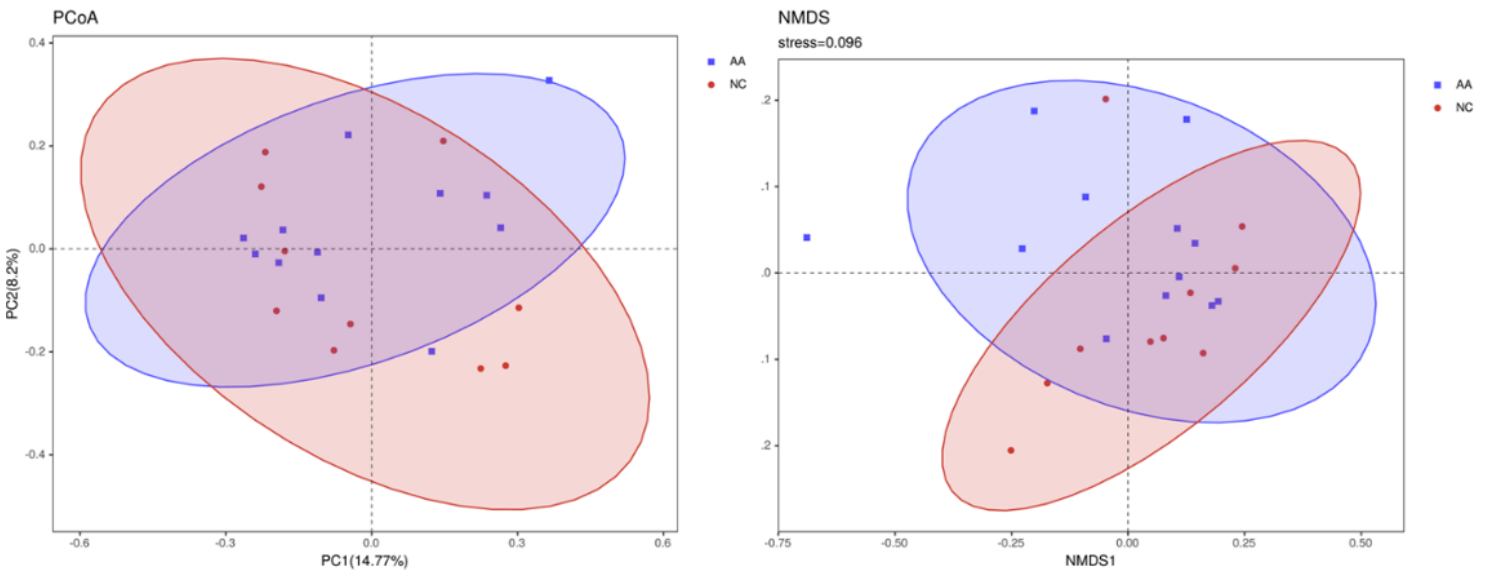

Figure 5

PCoA and NMDS analysis showed no significant community differences between AA and NC groups

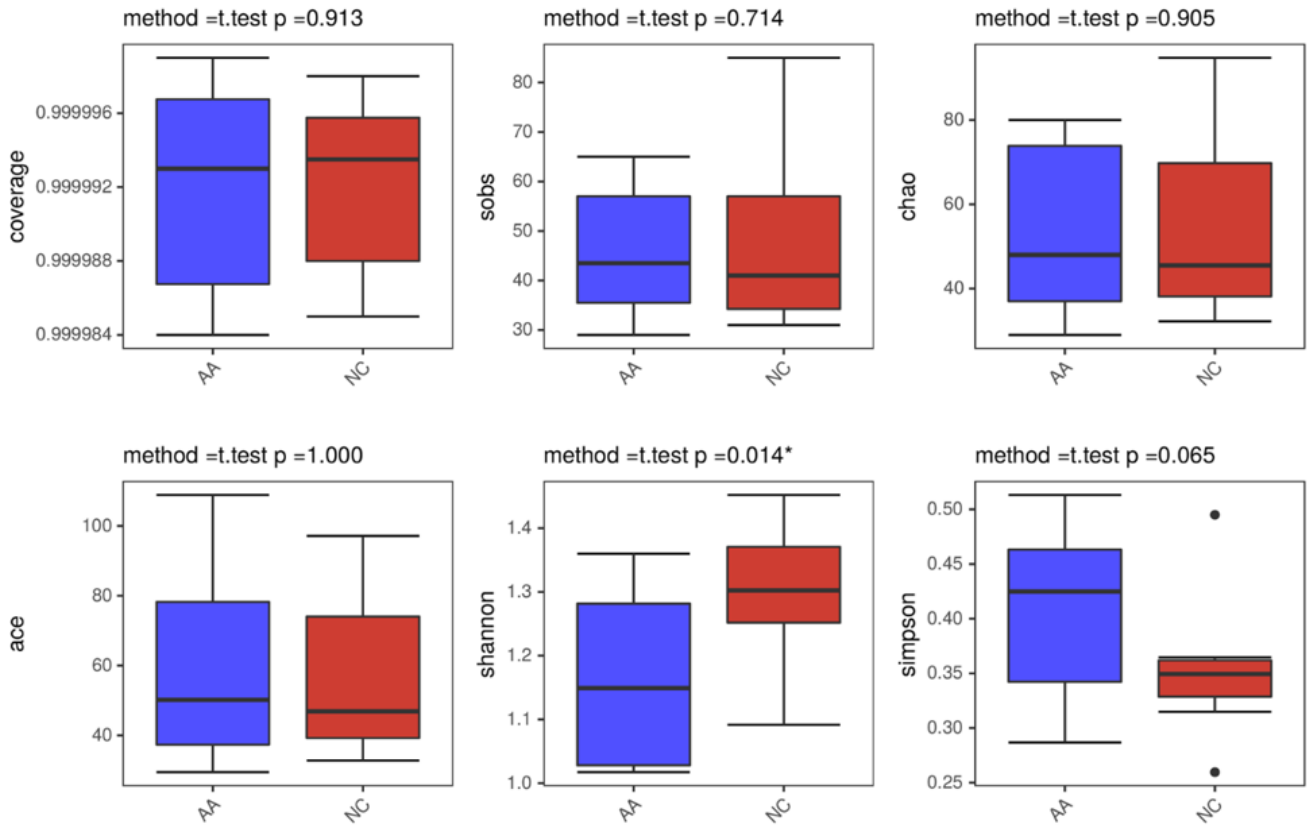

Figure 6

α diversity analysis in phylum level between the NC and AA groups, only the Shannon index shows the significant difference.

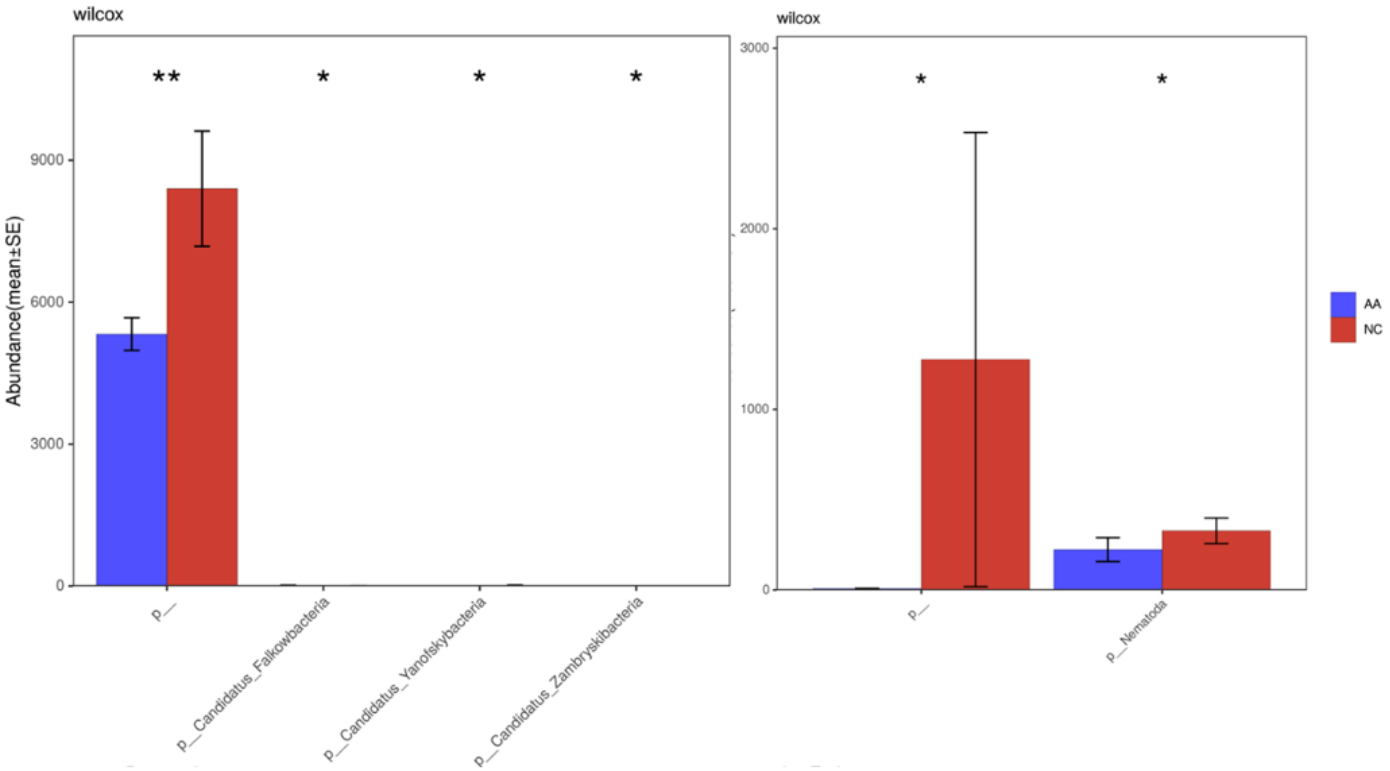

Figure 7

a.the changed bacterial abundance of AA patients in the phylum level. b. the changed eukaryote abundance of AA patients in the phylum level.

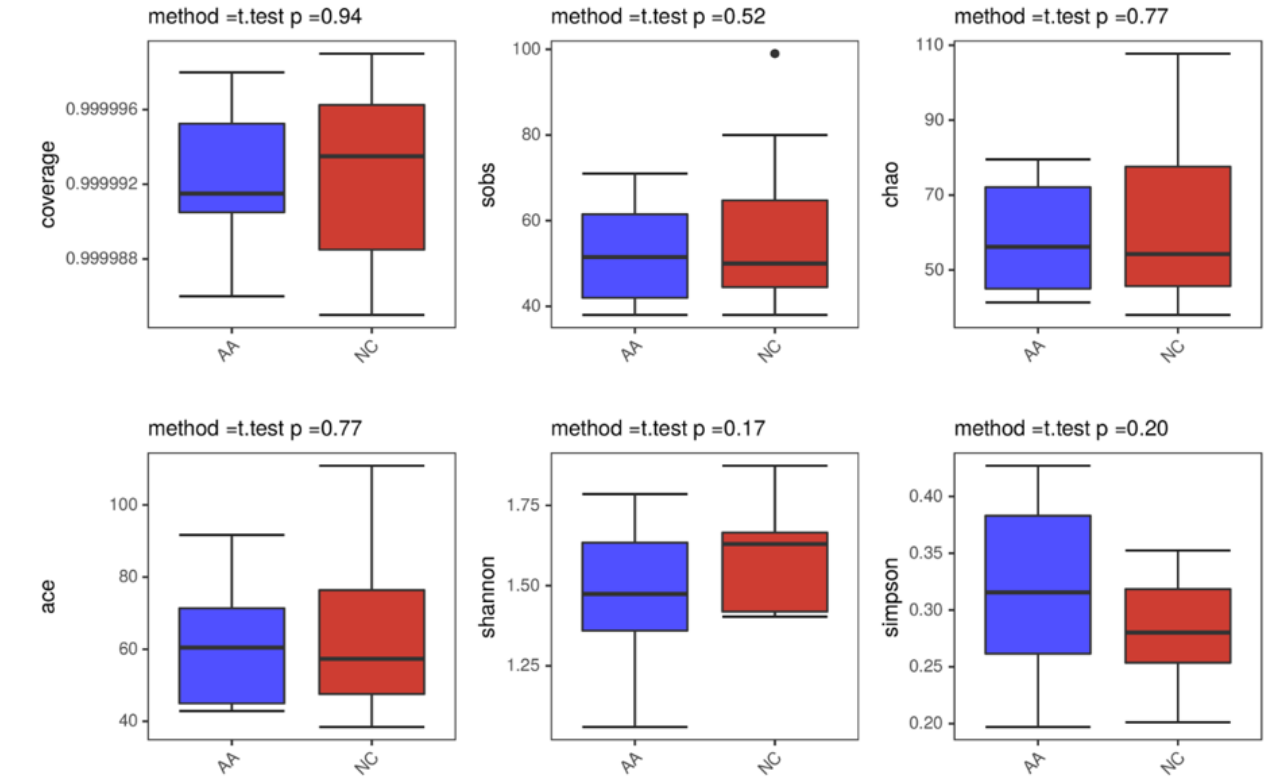

Figure 8

α diversity analysis in class level between the NC and AA groups, no index shows the significant difference.

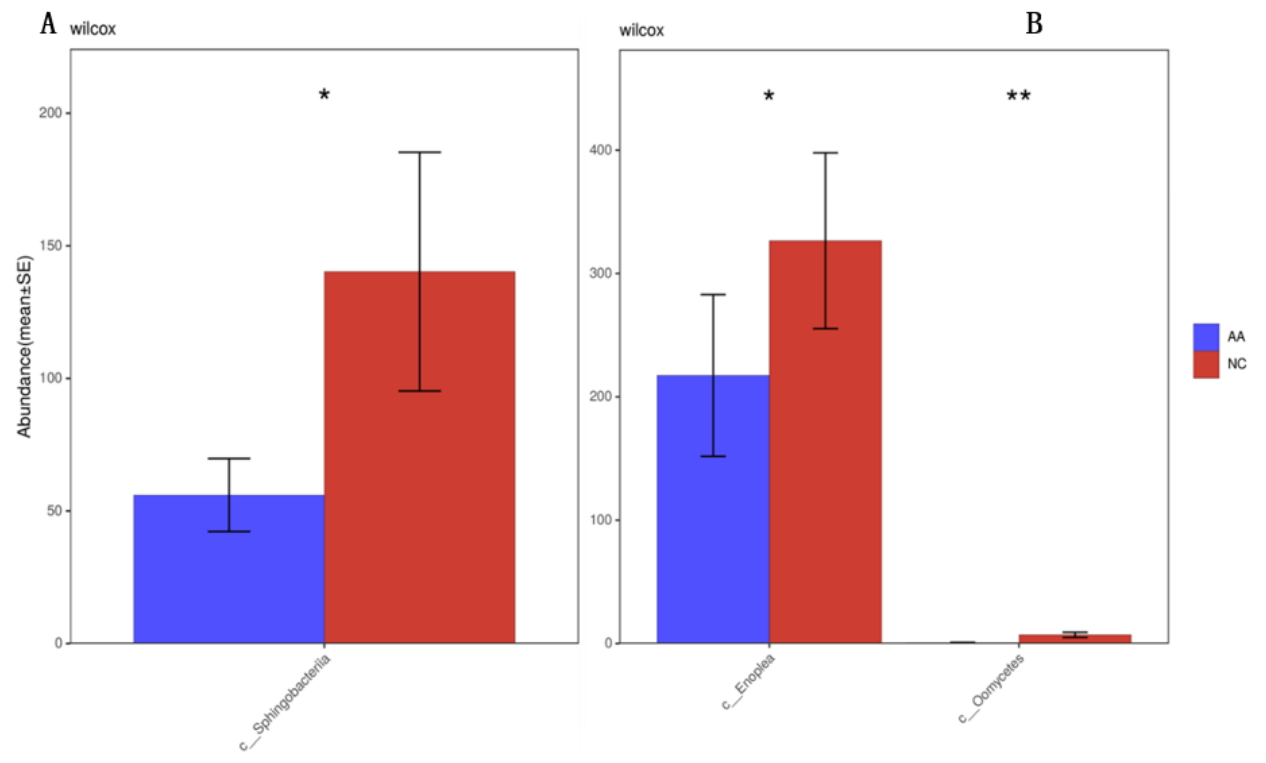

Figure 9

A. the changed bacterial abundance of AA patients in the class level. B. the changed eukaryote abundance of AA patients in the class level.

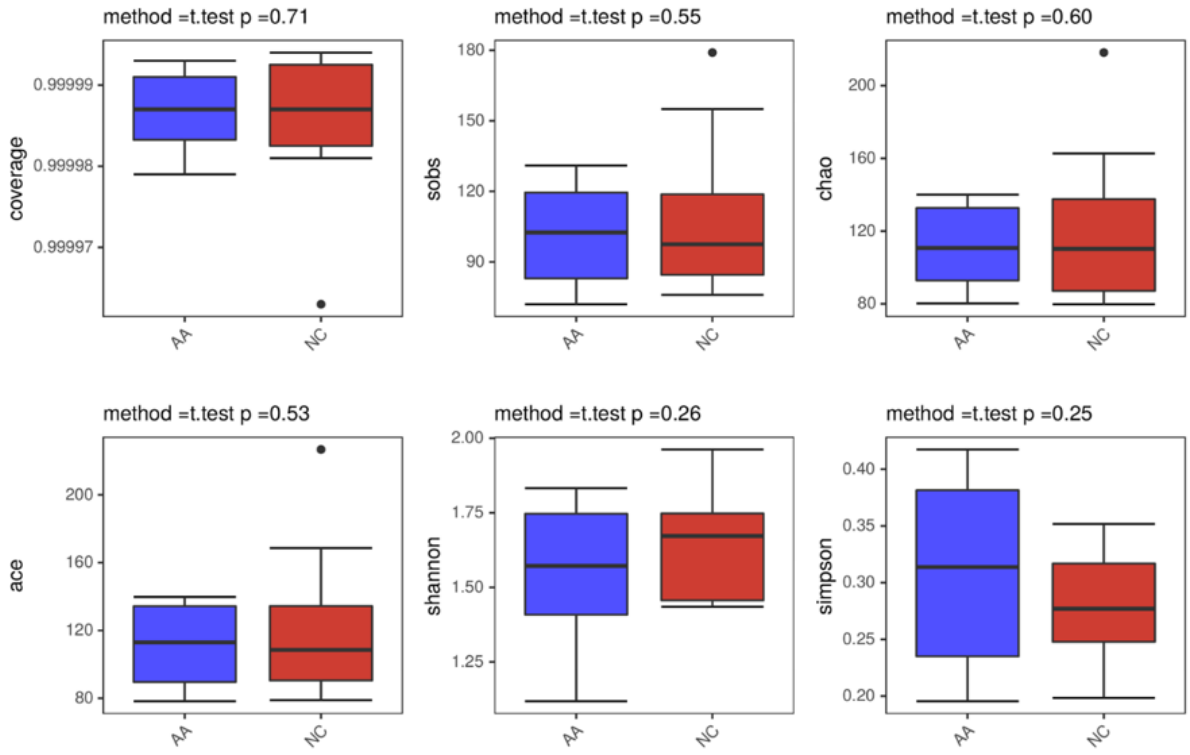

Figure 10

α diversity analysis in order level between the NC and AA groups, no index shows the significant difference.

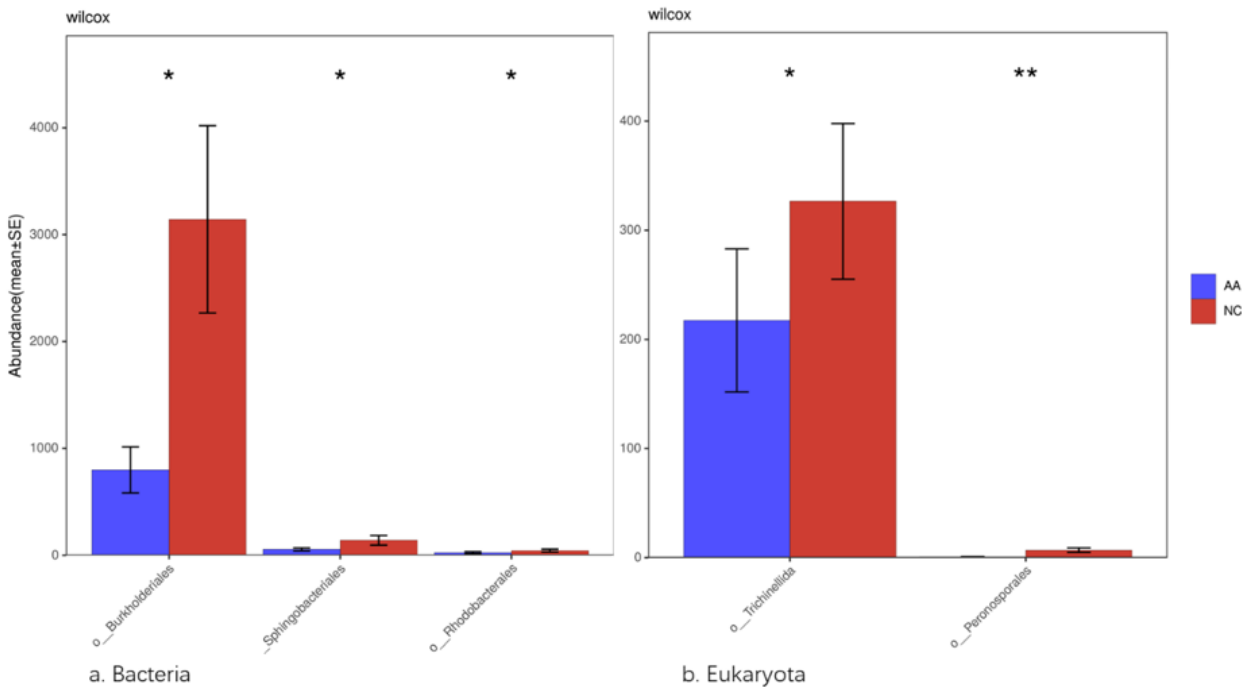

Figure 11

a. the changed bacterial abundance of AA patients in the order level. b. the changed eukaryote abundance of AA patients in the order level.

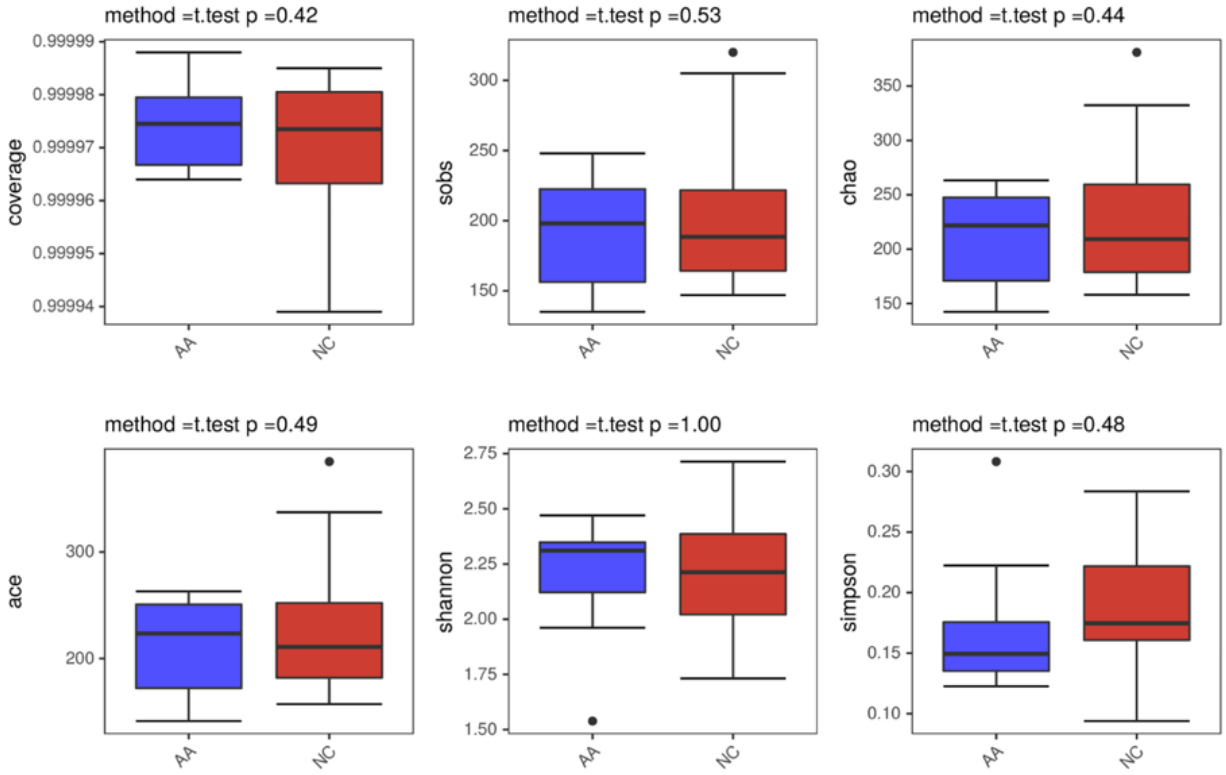

Figure 12

α diversity analysis in family level between the NC and AA groups, no index shows the significant difference

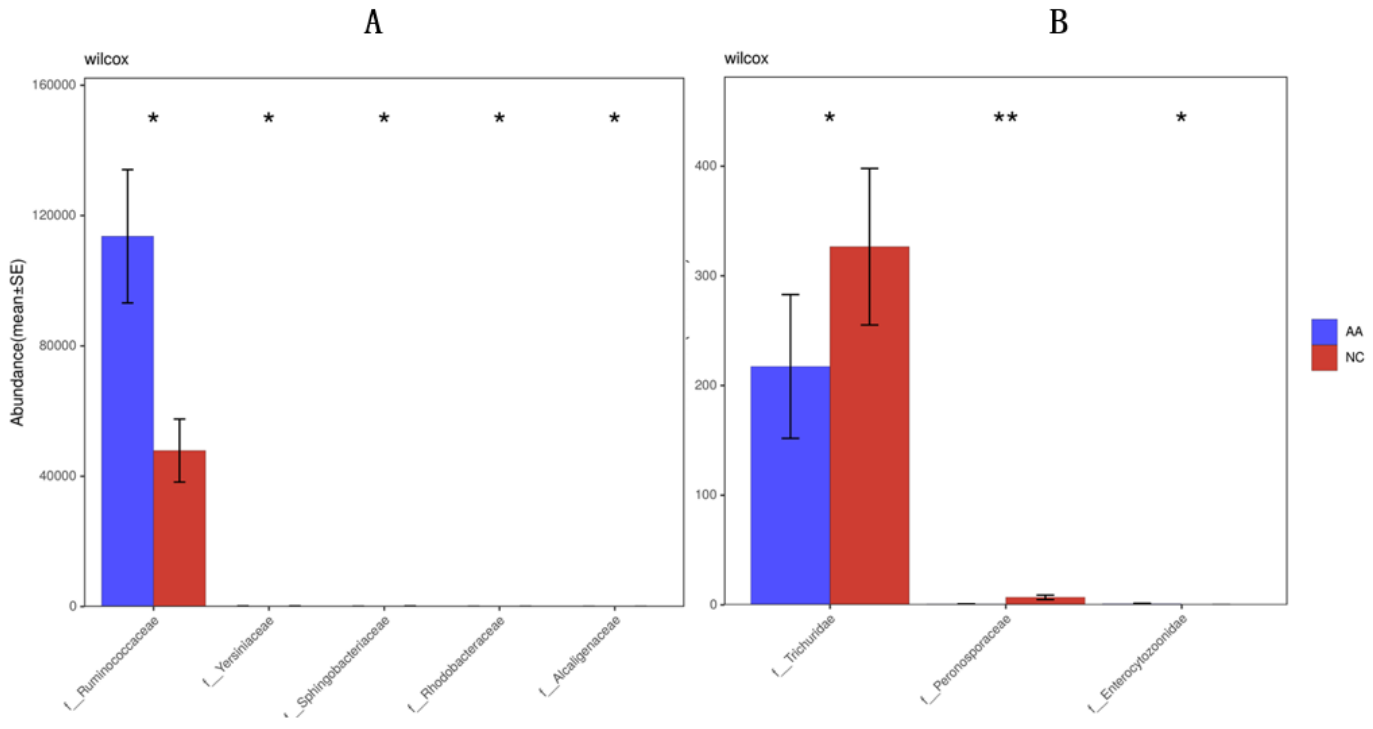

Figure 13

A. the changed bacterial abundance of AA patients in the family level. B. the changed eukaryote abundance of AA patients in the family level.

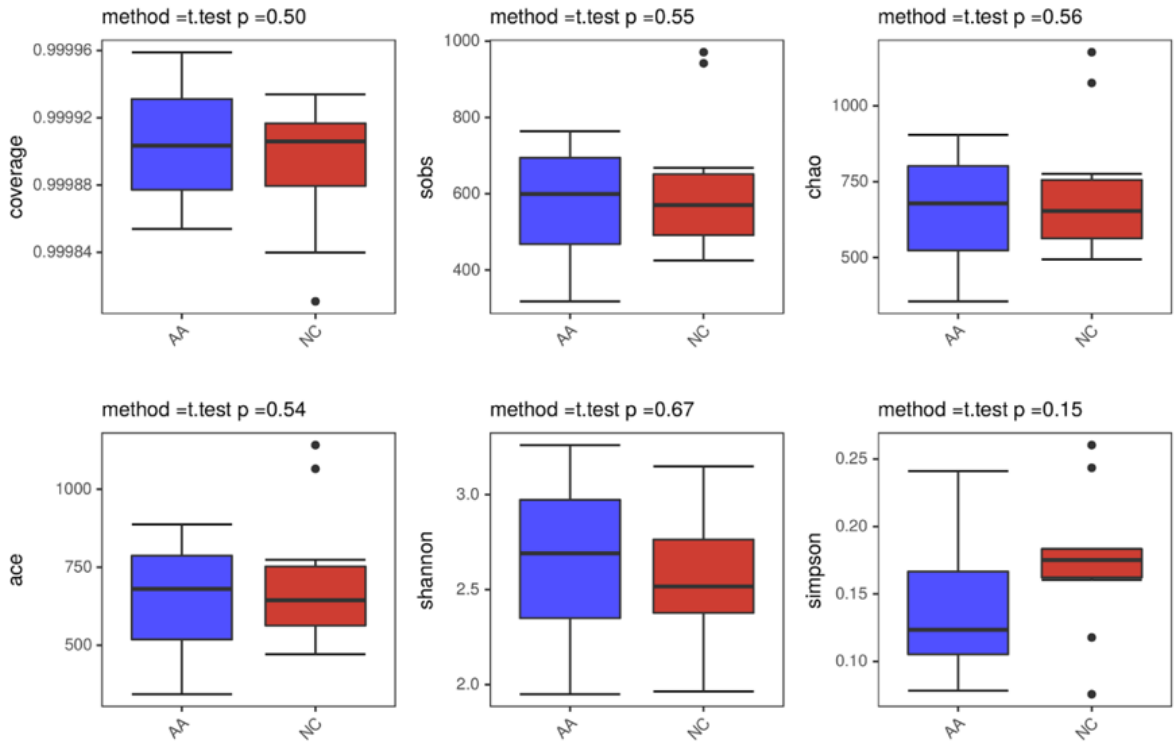

Figure 14

α diversity analysis in family level between the NC and AA groups, no index shows the significant difference

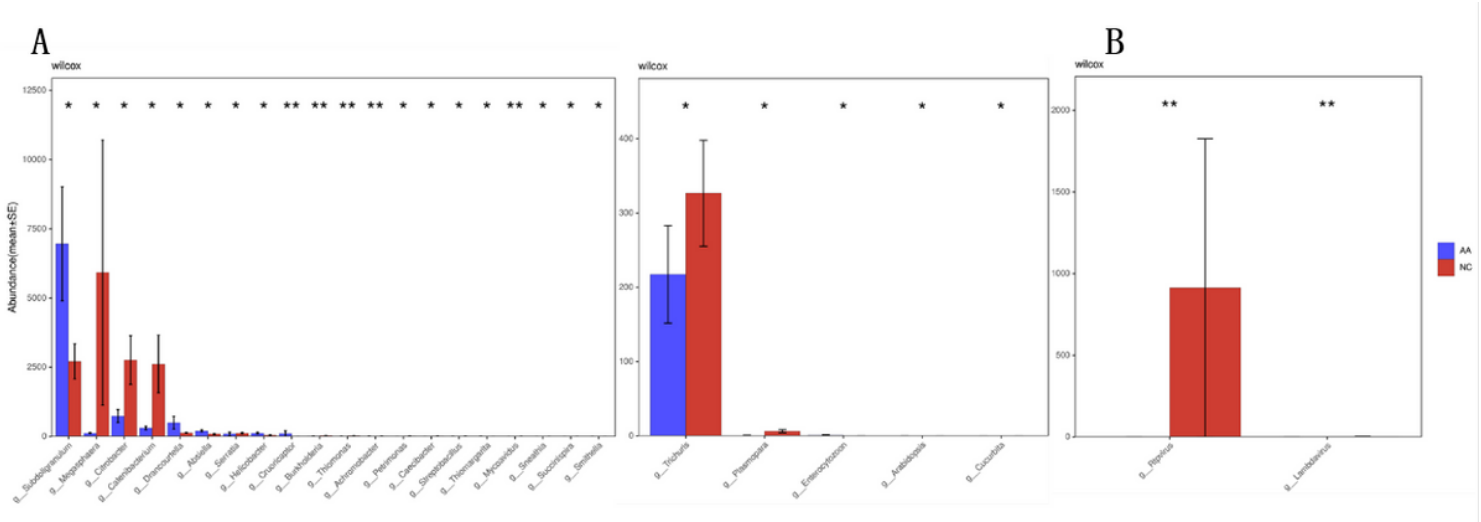

Figure 15

A. the changed bacterial abundance of AA patients in the genus level. B. the changed eukaryote abundance of AA patients in the genus level. C. the changed virus abundance of AA patients in the genus level.

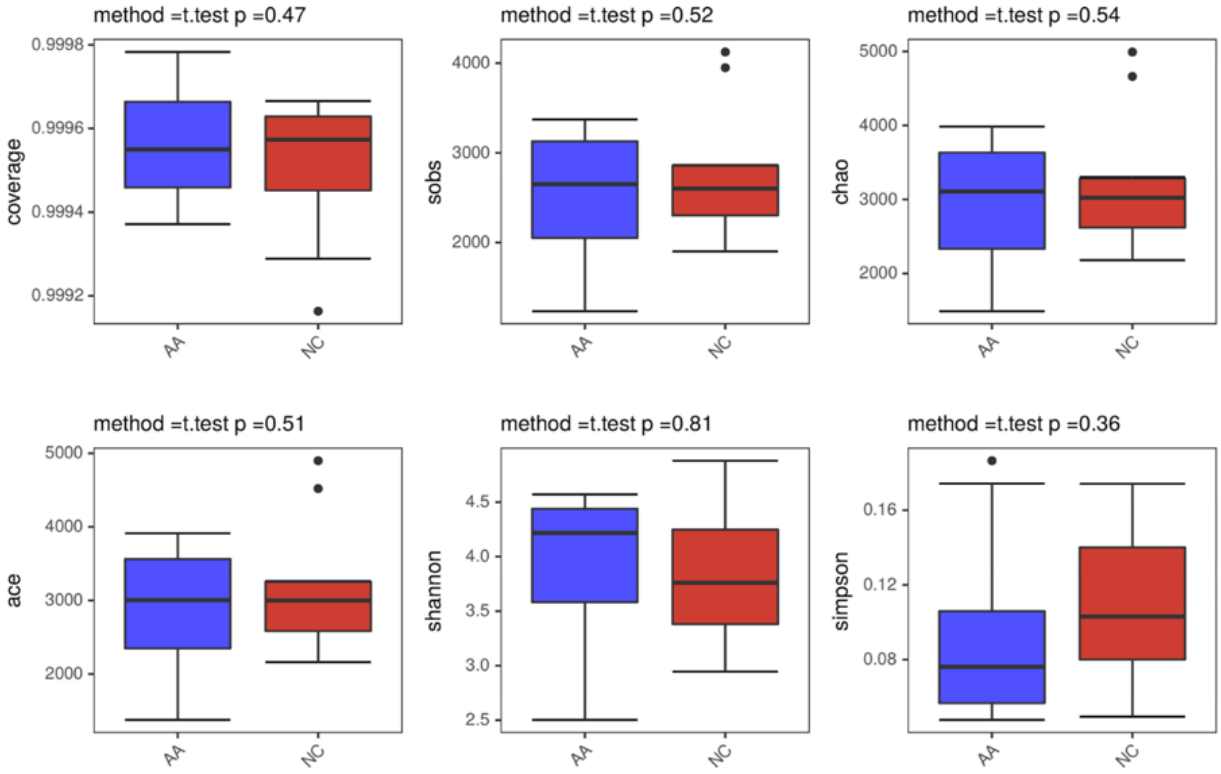

Figure 16

α diversity analysis in family level between the NC and AA groups, no index shows the significant difference

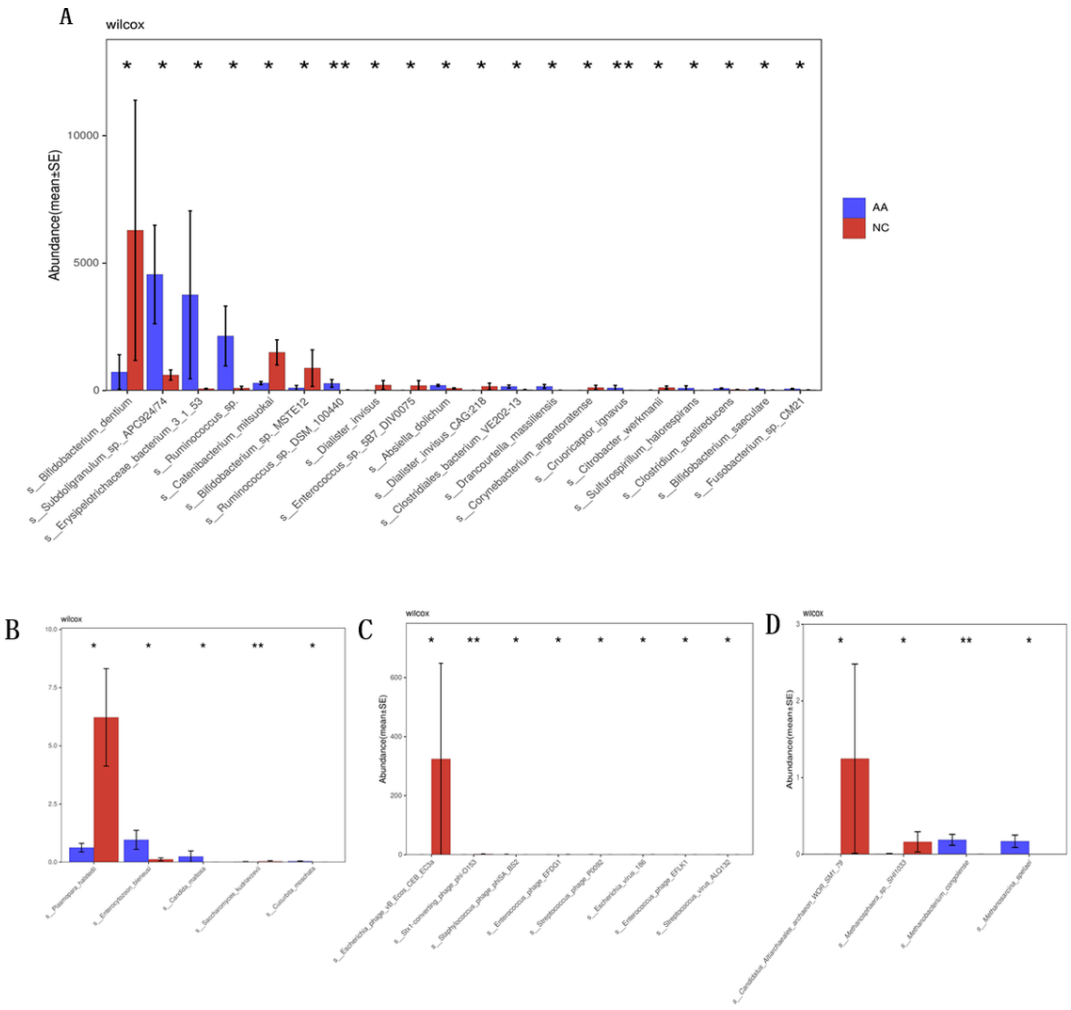

Figure 17

A. the changed bacterial abundance of AA patients in the species level. B. the changed eukaryote abundance of AA patients in the species level. C. the changed virus abundance of AA patients in the species level. D. the changed archaea abundance of AA patients in the species level.

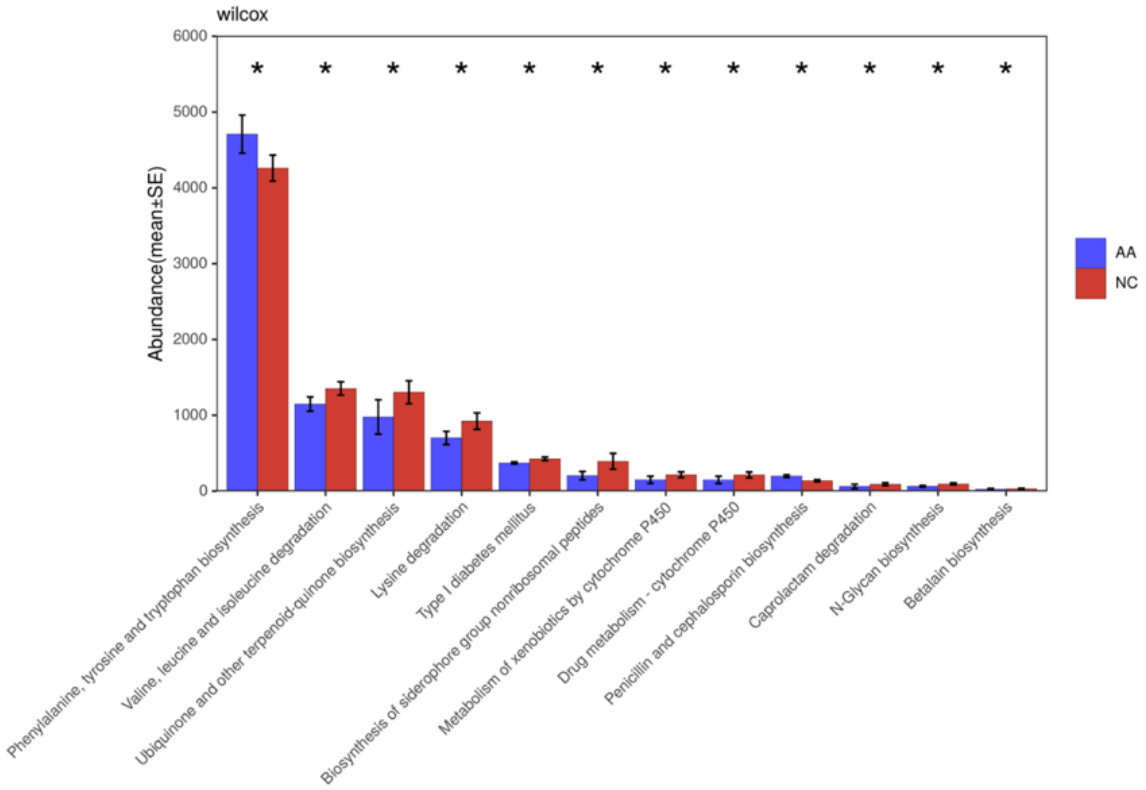

Figure 18

Changed abundance of KEGG pathway in AA group

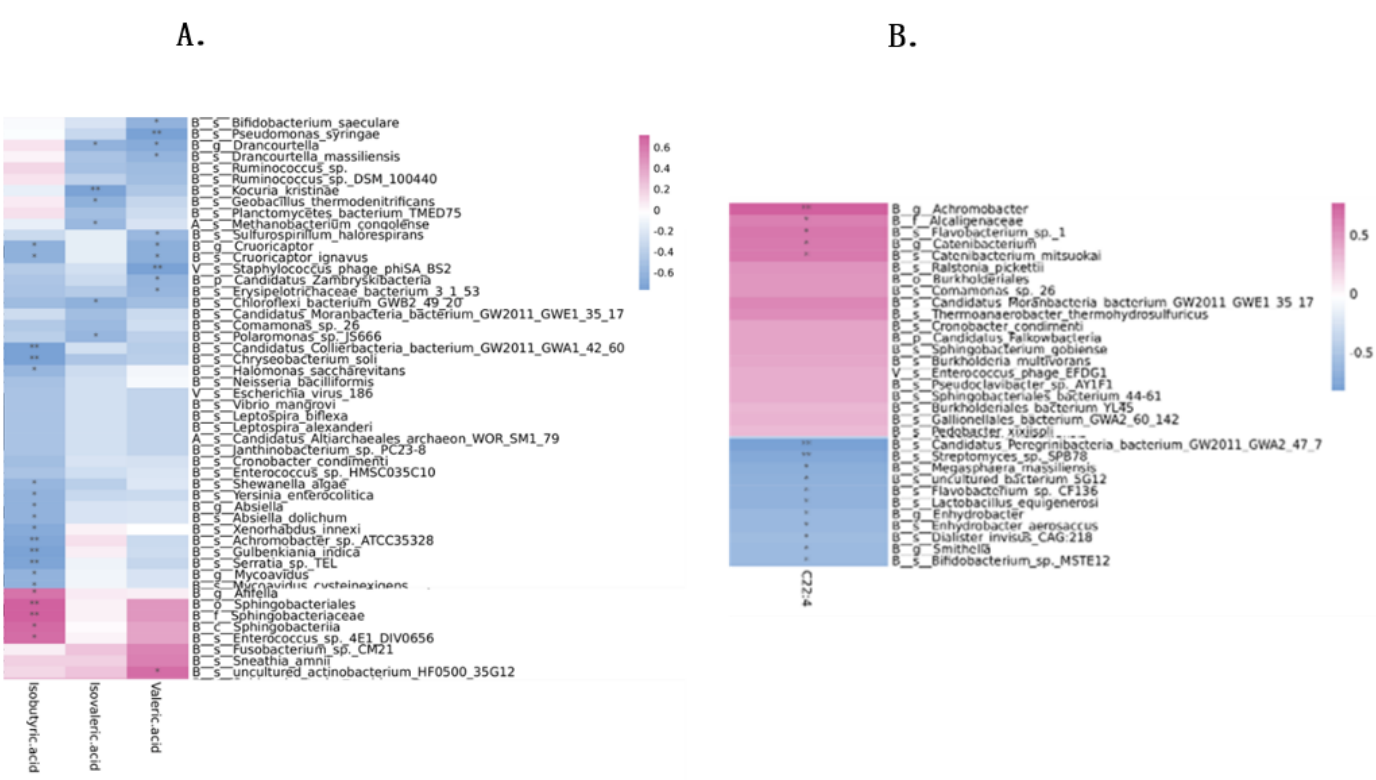

Figure 19

A.the correlation between microbial abundance and short-chain fatty acids in the bone marrow supernatant in AA group. B. the correlation between microbial abundance and long-chain fatty acids in the bone marrow supernatant in AA group. (only the significant correlation showed here)

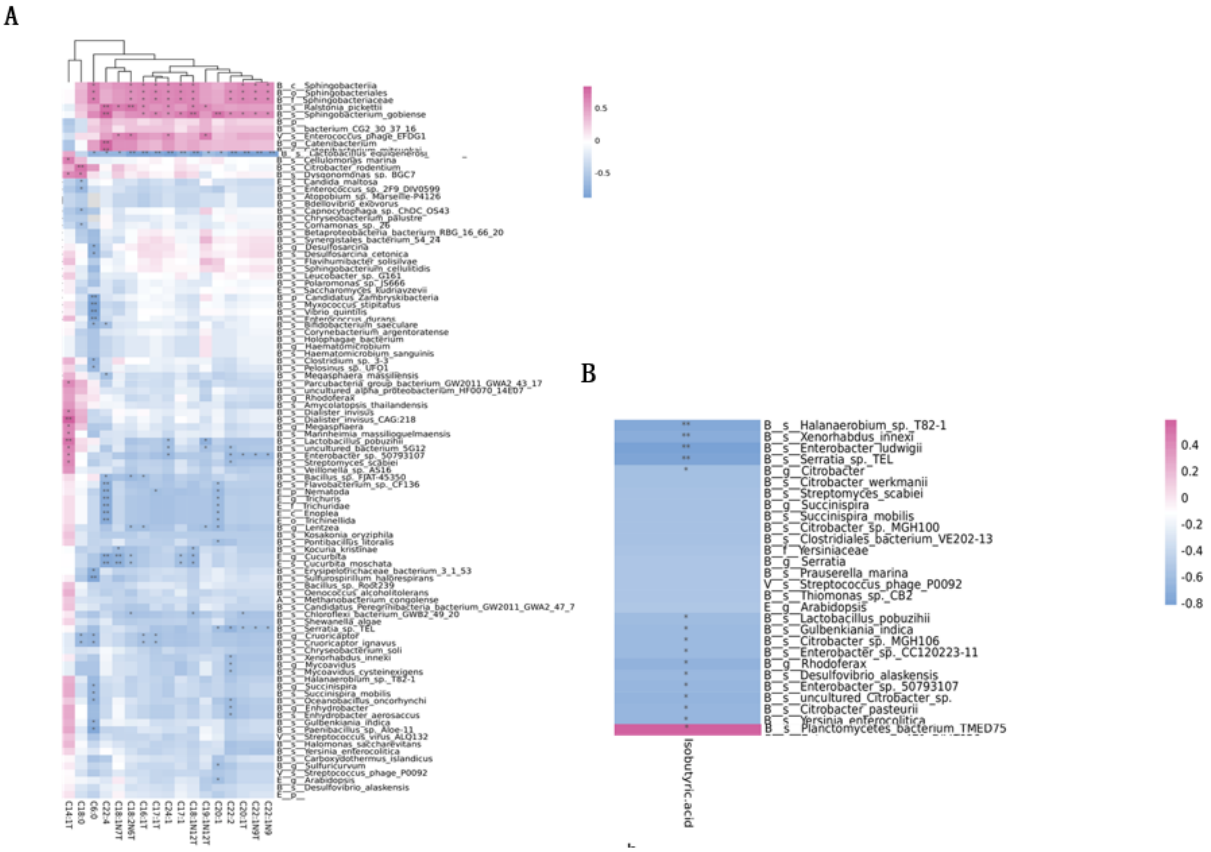

Figure 20

A. the correlation between microbial abundance and long-chain fatty acids in the plasm in AA group. B. the correlation between microbial abundance and ahort-chain fatty acids in the plasm in AA group. (only the significant correlation showed here)

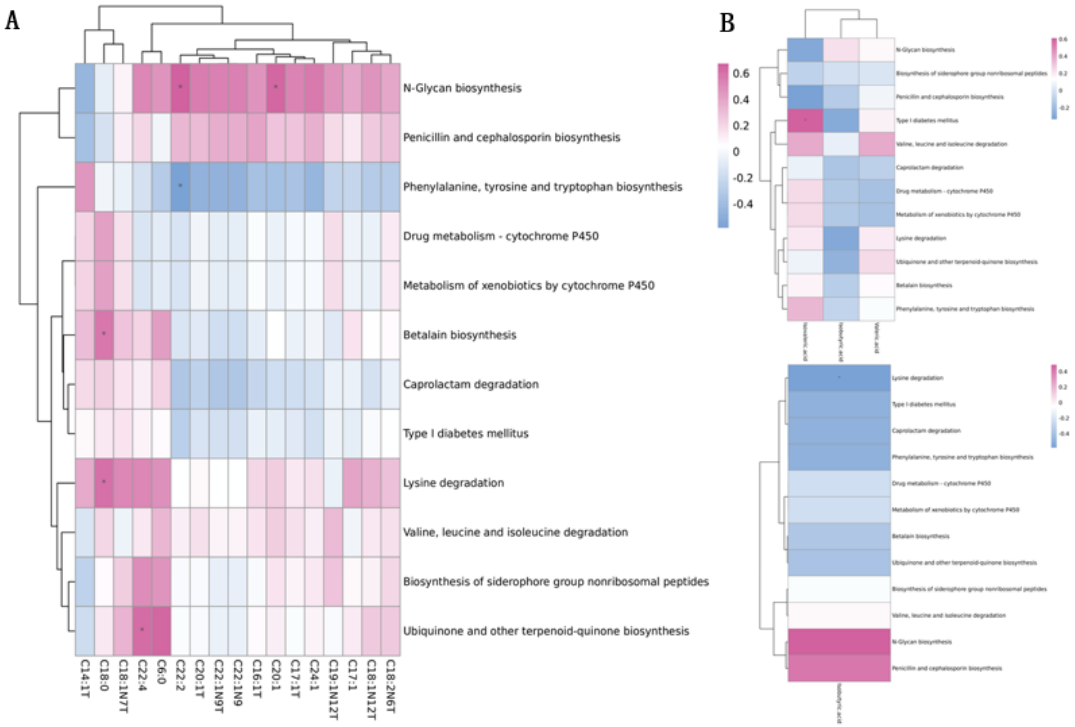

Figure 21

A.the correlation between the abundance of KEGG pathway and the long-chain fatty acids. B. the correlation between abundance of KEGG pathway and the short-chain fatty acids

Figure 22

the correlation between the microbial abundance and the KEGG pathway abundance.

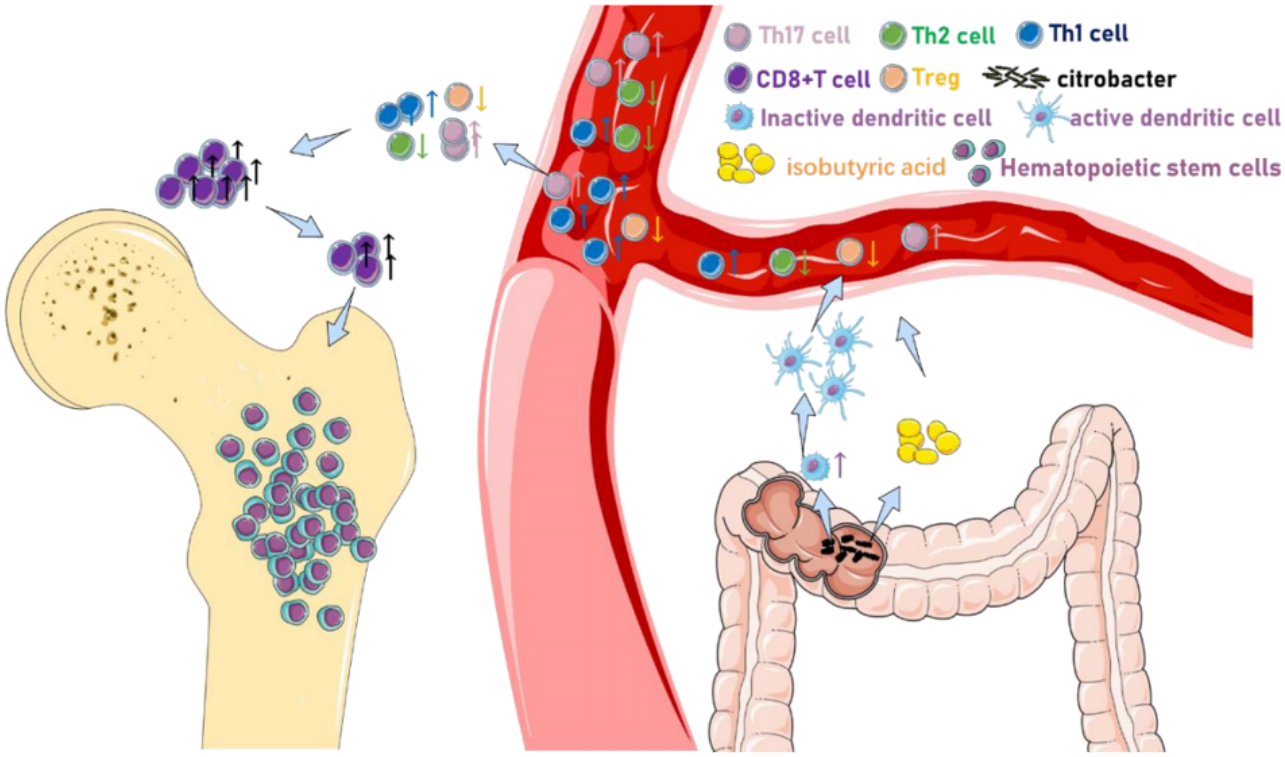

Figure 23

Citrobacter infection may affect the immune status of the body directly or by adjusting the content of isobutyric acid in the intestines, thereby inducing aplastic anemia.